



City Research Online

City, University of London Institutional Repository

Citation: Chappell, D. C. (1991). Fluorescent labelling of proteins - Volume 2.
(Unpublished Doctoral thesis, City, University of London)

This is the accepted version of the paper.

This version of the publication may differ from the final published version.

Permanent repository link: <https://openaccess.city.ac.uk/id/eprint/28492/>

Link to published version:

Copyright: City Research Online aims to make research outputs of City, University of London available to a wider audience. Copyright and Moral Rights remain with the author(s) and/or copyright holders. URLs from City Research Online may be freely distributed and linked to.

Reuse: Copies of full items can be used for personal research or study, educational, or not-for-profit purposes without prior permission or charge. Provided that the authors, title and full bibliographic details are credited, a hyperlink and/or URL is given for the original metadata page and the content is not changed in any way.

FLUORESCENT
LABELLING
OF PROTEINS

VOLUME 2.

by

DAVID CLIVE CHAPPELL

A thesis submitted for the Degree of
DOCTOR OF PHILOSOPHY
in the Chemistry Department of
The City University, London.

April, 1991.

CHAPTER 7 - INVESTIGATION INTO THE AGGREGATION OF TETRAMETHYLRHODAMINE IN AQUEOUS SOLUTION, AND ITS FLUORESCENCE QUENCHING ACTION ON THE EMISSION OF FLUORESCHEIN	1
7.1 Introduction to Fluorescence Quenching	1
7.1.1 Dynamic Quenching	1
7.1.2 Static Quenching	3
7.1.3 Combined Dynamic and Static Quenching	4
7.1.4 Quenchers of Fluorescence	5
7.1.5 Fluorescence Quenching Via Energy Transfer	6
7.1.6 Distance Measurements by Energy Transfer	8
7.2 Self-Association of Dyes in Aqueous Solution	10
7.2.1 Fluorescent Modification of Proteins Utilising TRITC and FITC	11
7.2.1.1 Experimental Procedure	12
7.2.1.2 Results for Free TRITC and its Protein Conjugates both in the Presence and Absence of SDS	15
7.2.1.3 Results for Free TRITC and its Protein Conjugates both in the Presence and Absence of SDS	17
7.2.1.4 Summary of Results	18
7.2.1.5 Stoichiometry of Labelling	20
7.2.1.6 Calculation of the Stoichiometry of Labelling for TRITC/anti-G1gG	21
7.2.2 Effect of Removal of SDS from the TRITC-Protein Conjugates	23
7.2.2.1 Experimental Procedure	23
7.2.2.2 Results	23
7.2.2.3 Summary of Results	24
7.2.3 Investigation of the Action of Urea, 2-mercaptoethanol and SDS on Commercial TRITC-Protein Conjugates	24
7.2.3.1 Experimental Procedure	24
7.2.3.2 Results	25
7.2.3.3 Stoichiometry of Labelling of the Commercial Conjugates	26
7.2.3.4 Summary of Results	26
7.2.4 Investigation of the Interaction Between Free TRITC and Free FITC as well as Their Protein Conjugates and SDS, as Detected by fluorescence Spectroscopy	27

7.2.4.1	Experimental Procedure for the Fluorescent Modification of Proteins Utilising TRITC and FITC	27
7.2.4.2	Results for Free TRITC and its Protein Conjugates	28
7.2.4.3	Results for Free FITC and its Protein Conjugates	30
7.2.4.4	Summary of Results	32
7.2.4.5	Conclusion	34
7.3	Further Investigations into the Self-Association Process	37
7.3.1	The Preparation of the TRITC-Glycine Conjugate	37
7.3.1.1	Experimental Procedure	37
7.3.1.2	Results	38
7.3.1.3	Summary of Results	38
7.3.2	Investigation of the Non-specific Binding of Fluorescein to anti-RIG and anti-GIG	40
7.3.2.1	Experimental Procedure	40
7.3.2.2	Results	41
7.3.2.3	Summary of Results	42
7.3.2.4	Conclusion	43
7.4	Investigation into the Process of Resonance Energy Transfer from Fluorescein to Tetramethylrhodamine, as Analysed by Absorption Spectroscopy	46
7.4.1	Experimental Procedure	46
7.4.2	Results	47
7.4.3	Summary of Results	49
7.5	Investigation into the Fluorescence Quenching of Tetramethylrhodamine by Fluorescein, as Analysed by Fluorescence Spectroscopy	49
7.5.1	Experimental Procedure	50
7.5.2	Results	50
7.5.3	Summary of Results	53
7.5.4	Conclusion	55
7.6	References	
CHAPTER 8 - INVESTIGATION INTO THE NATURE OF THE FLUORESCENCE QUENCHING OF AN EXTRINSIC FLUOROPHORE BY THE HAEM MOIETY IN HORSERADISH PEROXIDASE		57
8.1	Discovery of Horseradish Peroxidase	57

8.2	Location, Isolation and Purification of Horseradish Peroxidase	57
8.3	Chemical and Physical Properties of Horseradish Peroxidase	58
8.4	Primary Structure of HRP	61
8.5	Homology Between HRP-C and Other Haemoproteins	62
8.6	The Secondary Structure of HRP	64
8.7	Function and Mechanism of Action of HRP	66
8.8	Fluorescent Modification of HRP-C Using FITC	70
8.8.1	Experimental Procedure	71
8.8.2	Results	72
8.8.3	Calculation of the Stoichiometry of the FITC/HRP-C Conjugate	73
8.8.4	Summary of Results	73
8.9	Correlation Between the RZ Value of the Protein and the Extent of Fluorescence Quenching of Ru Complex I	74
8.9.1	Experimental Procedure	74
8.9.2	Results	74
8.9.3	Conclusion	75
8.10	Determination of the Distance Between the Haem Moiety and the Covalent Fluorophore	76
8.10.1	Experimental Procedure	79
8.10.2	Results	79
8.10.3	Conclusion	81
8.11	Determination of the Position of the Reactive Lysine Residue Via Affinity Chromatography	81
8.11.1	Principle of Technique	81
8.11.2	Experimental Procedure	84
8.11.3	Results	86
8.11.4	Conclusion	89
8.12	Summary	91
8.13	References	
	APPENDIX - EXPERIMENTAL DETAILS	92

ABSTRACT

Investigations were also undertaken in order to gain a fuller understanding of the process of fluorescence quenching via resonance energy transfer. In order to achieve this, tetramethylrhodamine dimers and fluorescein dimers were produced in aqueous solution, whereby excited state energy from the fluorescein chromophore is donated to the tetramethylrhodamine chromophore. Also, a series of proteins were fluorescently modified via lysine residues with these reagents, and the resultant absorption and fluorescence spectra were examined.

A natural fluorescence quencher of both intrinsic and extrinsic fluorescent species is the haem moiety of the haemoproteins. Horseradish peroxidase isoenzyme C, was investigated with regard to its efficiency in this respect. Partial fluorescent modification of the enzyme was achieved, utilising amine-reactive fluorescein and organometallic chromophores, as the extrinsic fluorescent species. The distance between the haem centre and the respective fluorophore was calculated, and the position of the reactive lysine residue was suggested.

CHAPTER 7.

INVESTIGATION INTO THE AGGREGATION OF TETRAMETHYL RHODAMINE
IN AQUEOUS SOLUTION AND ITS FLUORESCENCE QUENCHING
ACTION ON THE EMISSION OF FLUORESCHEIN.

7.1. INTRODUCTION TO FLUORESCENCE QUENCHING.

Fluorescence quenching refers to any process which decreases the fluorescence intensity of a given substance. A variety of processes can result in fluorescence quenching; these include excited state reactions, collisional or dynamic quenching and complex formation that can occur purely in the excited state: $M^* + M \longrightarrow (MM)^*$, which is also referred to as static quenching when there is association in the ground state: $(MM) \xrightarrow{h\nu} (MM)^*$.

7.1.1. Dynamic Quenching.

In order for dynamic quenching to occur, the quencher must diffuse to the fluorophore, during the lifetime of the excited state. Upon interaction, the fluorophore returns to the ground state, without emission of a photon. As a consequence, the fluorophore and quencher must be in close proximity. It is this requirement which allows fluorescence quenching to be utilised for numerous investigations. For example, quenching measurements can reveal the accessibility of fluorophores to quenchers. If the fluorophore and quencher are present in a solvent of high viscosity; then diffusion is slow, and quenching is inhibited. Thus, quenching can yield information regarding the diffusion rates of quenchers. Moreover, if a fluorophore is bound to the interior of a membrane and the latter is impermeable to the quencher, then dynamic quenching may not occur. As a consequence, quenching studies may be used to reveal the localisation of fluorophores, and their permeabilities to quenchers.

An important aspect of dynamic quenching, is the expansion of the volume and the distance within the solution between the fluorophore and quencher; which may affect the fluorescence intensity or the lifetime of the excited state of the fluorophore.

The root mean square distance over which the quencher can diffuse during the lifetime of the excited state, is given by twice the product of the lifetime of the excited state (T) and the diffusion coefficient (D).

$$(\Delta x^2)^{\frac{1}{2}} = 2DT$$

Dynamic quenching of fluorescence is described by the Stern-Volmer equation:

$$F_0/F = 1 + K_q T_0 [Q] = 1 + K_D [Q]$$

where F_0 and F are the fluorescence intensities in the absence and presence of quencher, respectively; K_q is the bimolecular quenching constant; T_0 is the lifetime of the fluorophore in the absence of quencher; $[Q]$ is the concentration of the quencher; and $K_D = K_q T_0$ is the Stern-Volmer quenching constant.

Quenching data are frequently presented as a plot of F_0/F against $[Q]$. This plot is called a Stern-Volmer plot and should describe a straight line, since F_0/F is expected to be linearly dependent upon the concentration of the quencher. The Stern-Volmer plot yields an intercept of one on the y axis, and a slope equal to the Stern-Volmer quenching constant, K_D .

K_D^{-1} is the quencher concentration at which $F_0/F = 2$, or 50% of the intensity is quenched.

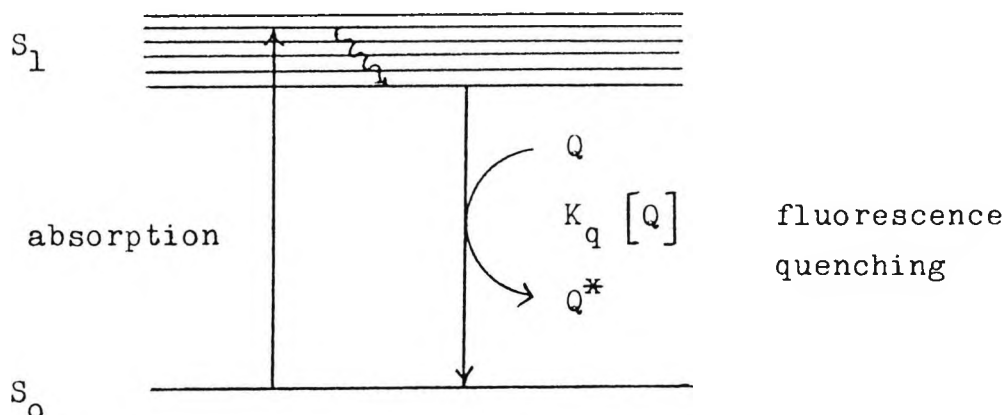


Fig. 7.1. Schematic diagram of the process of Dynamic Quenching of a Fluorophore. The quencher, Q, combines with the excited state fluorophore on its return to the ground state, thereby quenching the fluorescence emission.

7.1.2. Static Quenching.

Quenching may also occur as a result of the formation of a non-fluorescent ground state complex, between the fluorophore and quencher. When this complex absorbs light, it immediately returns to the ground state without emission of a photon.

A plot of F_0/F against $[Q]$ is also linear with an intercept on the y axis of one, and a slope equal to K_s which is the association constant.

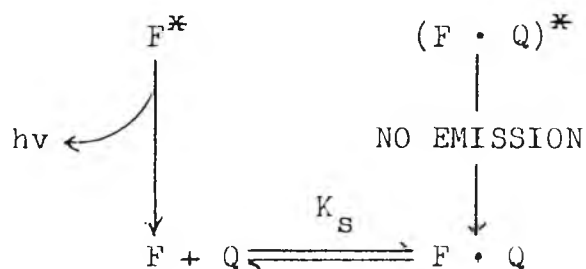


Fig. 7.2. Schematic diagram of the process of Static Quenching of a Fluorophore. F^* and $(F \cdot Q)^*$ are excited state fluorophore and fluorophore-quencher complex respectively.

Fluorescence quenching data, obtained by intensity measurements alone, can be explained by either dynamic or static quenching processes unless additional information is provided. The measurement of fluorescence lifetimes is the most definitive method to distinguish static and dynamic quenching. Static quenching removes a fraction of the fluorophores from observation. The complexed fluorophores are usually non-fluorescent and only observed fluorescence is from the uncomplexed fluorophore. The uncomplexed fraction is unperturbed, and hence the lifetime is T_0 . Therefore, for static quenching, $T_0/T = 1$. For dynamic quenching, there is an equivalent decrease in the fluorescence intensity and lifetime, therefore, $T_0/T = F_0/F$.

An additional method to distinguish between static and dynamic quenching, is by careful examination of the absorption spectrum of the fluorophore. Dynamic quenching only affects the excited states of the fluorophores, and thus no changes in the absorption spectrum are predicted. In contrast, ground state complex formation will frequently result in perturbation of the absorption spectrum of the fluorophore.

7.1.3. Combined Dynamic and Static Quenching.

In many instances the fluorophore can be quenched, both by collisions and by complex formation with the same quencher. The characteristic feature of the Stern-Volmer plots, in such circumstances, is an upward curvature, concave towards the y axis.

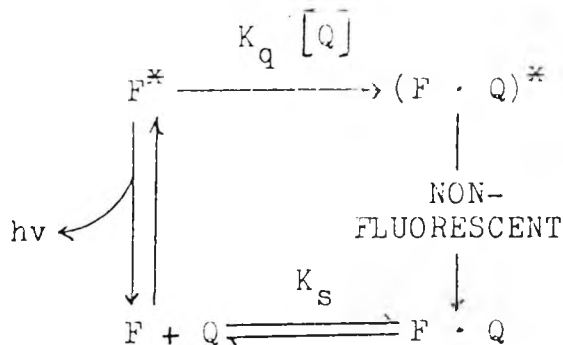


Fig. 7.3. Schematic diagram of the interrelation between the processes of dynamic and static quenching.

7.1.4. Quenchers of Fluorescence.

One of the best known dynamic quenchers is molecular oxygen (1), which quenches almost all known fluorophores. It is frequently necessary to remove dissolved oxygen, to obtain reliable measurements of the fluorescence yields and lifetimes, and it is clear that contact between the oxygen molecule and the fluorophore, is a requirement for quenching.

Aromatic and aliphatic tertiary amines are efficient quenchers of most unsubstituted aromatic hydrocarbons (2); fluorescence is effectively quenched by diethylaniline. In this instance, the mechanism of quenching is the formation of a charge transfer complex. The excited state fluorophore accepts an electron from the amine. In non-polar solvents, fluorescence emission from the charge-transfer complex (exciplex) is frequently observed, and this process may be regarded as an excited state reaction rather than quenching. In polar solvents, the exciplex emission is often quenched, so that the fluorophore-amine interaction appears to be that of simple quenching. Other dynamic quenchers include the iodide anion (3), xenon (4), hydrogen peroxide (5), perbromate

anion (6), nitromethane (7), nitroxides (8) and olefins (9,10). Quenching by the larger halogens, such as bromide and iodide, may be a result of intersystem crossing to an excited triplet state, promoted by spin-orbit coupling of the excited (singlet) fluorophore, and the halogen (11). Since emission from the triplet state is slow, this emission is highly quenched by other processes. Also many halogen-containing substances act as dynamic quenchers. These include substances such as bromobenzene (12), chloroform, trichloroethanol (13) and methylmercuric chloride (14).

Not all fluorophores are quenched by all of the substances mentioned. This fact allows the selective quenching of a given fluorophore. The occurrence of quenching depends upon the mechanism, which in turn, depends upon the structures of the individual molecules concerned.

7.1.5. Fluorescence Quenching Via Energy Transfer.

Another important means of fluorescence quenching, is via energy transfer. This process is the transfer of the excited state energy, from a donor (d) to an acceptor (a). This transfer occurs without the emission of a photon, and is primarily a result of dipole-dipole interactions between the donor and acceptor. The rate of energy transfer depends upon a number of factors:

- i) the extent of overlap of the emission spectrum of the donor, with the absorption spectrum of the acceptor;
- ii) the relative orientation of the donor and acceptor transition dipoles; and
- iii) the distance between the donor and acceptor molecules.

The rate of energy transfer (K_T), from a specific donor to a specific acceptor, is given by:

$$K_T = \frac{1}{T_d} \cdot \left(\frac{R_0}{r} \right)^6$$

where T_d is the lifetime of the donor in the absence of acceptor; r is the distance between the donor and acceptor; and R_0 is a characteristic distance, called the "Förster distance, at which the efficiency of transfer is 50% (15).

This dependence of the transfer rate on distance, has resulted in numerous applications of energy transfer in biochemical research. Any phenomenon which affects the donor-acceptor distance will affect the transfer rate, allowing the phenomenon to be quantified.

The "Förster distance, R_0 (in Å), may be determined by the following equation:

$$R_0 = 9.79 \times 10^3 \cdot (K^2 \cdot n^{-4} \cdot \phi_d \cdot J)^{1/6}$$

where K^2 is a factor describing the relative orientation in space of the transition dipoles of the donor and acceptor; n is the refractive index of the medium; ϕ_d is the quantum yield of the donor in the absence of acceptor; and J is the overlap integral which expresses the degree of spectral overlap between the donor emission and the acceptor absorption.

A frequently measured parameter is the efficiency of energy transfer (E), which is the proportion of photons absorbed by the donor, that are transferred to the acceptor.

$$E = \frac{K_T}{T_d^{-1} + K_T}$$

The transfer efficiency is frequently calculated from the relative fluorescence intensity in the presence (F_{da}), and absence of acceptor (F_d), or the lifetimes under these respective conditions (T_{da} and T_d).

$$E = 1 - (T_{da}/T_d)$$

$$E = 1 - (F_{da}/F_d)$$

The transfer efficiency may be directly related to the distance, using:

$$E = \frac{R_o^6}{R_o^6 + r^6}$$

7.1.6. Distance Measurements by Energy Transfer.

The photoreceptor protein of the disc membrane in vertebrate retinal rods, called rhodopsin, has been utilised (16) for fluorescence energy transfer experiments; in order to infer the shape of the protein, and the location of the binding sites on the protein. The chromophoric moiety of rhodopsin is 11-cis retinal. This chromophore isomerises upon light absorption, an event which signals the absorption of a photon. Retinal absorbs maximally at 500 nm, which is a favourable region to act as an energy acceptor for a wide variety of fluorophores.

Rhodopsin was labelled at three distinct sites (designated

A, B & C) with seven different fluorophores. Each of the fluorophores could donate energy to retinal, with R_0 values ranging from 33 to 51 Å. The efficiency of energy transfer was measured by both the lifetimes of the fluorophore (donor) in the absence (T_b) and presence (T_d) of acceptor, and by the relative quantum yields under these conditions, (Q_b and Q_d). The presence of acceptor is indicated by d, denoting dark. In the presence of light, retinal is bleached (b), eliminating its absorption band at 500 nm. Following bleaching of retinal, the lifetimes and yields of all donors increase. Essentially equivalent transfer efficiencies were obtained by both lifetimes and quantum yield measurements.

A conclusion from this study, is the large distance between site A and the retinal moiety, which was calculated to be 75 Å. If rhodopsin were a spherical molecule, its diameter could be no larger than 40-45 Å. Hence, the 75 Å distance between site A and the retinal site, indicates an elongated structure for the rhodopsin molecule. It was speculated that the three labelling sites are in a hydrophobic portion of rhodopsin, and that 11-cis retinal is located in a hydrophobic region which partitions in the membrane.

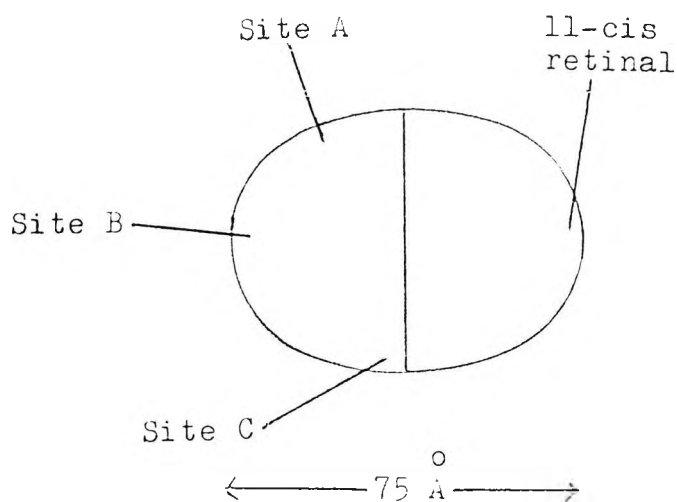


Fig. 7.4. Model of rhodopsin based on the observed distance between the sites (16).

There are many instances where the distance between the donor and acceptor molecules varies during the fluorescence lifetime of the donor. An example is the presence of a donor and acceptor molecule on either end of a flexible polypeptide chain. Thus, a range of end-to-end distances is expected. Time-dependent decays of donor fluorescence have been studied (17,18,19,20), in order to determine both the end-to-end distance probability distribution of a labelled polypeptide, and the diffusion coefficient for the end-to-end motion.

Energy transfer may also occur in solution, where donors and acceptors are each randomly distributed throughout the solution. Both the time-resolved decays of donor fluorescence and the relative quantum yields of the donor, are complex functions of the acceptor concentration. Those donors with nearby acceptors decay more rapidly, and donors more distant from acceptors decay more slowly. Thus, fluorescence quenching of a donor molecule by an acceptor molecule may occur in a variety of ways, and each method has been exploited for the investigation of various phenomena.

7.2. SELF-ASSOCIATION OF DYES IN AQUEOUS SOLUTION.

It is known that solutions of certain dyes in polar organic solvents at room temperature, follow Beer's law over an extended concentration range, but that in water, large deviations from the law are observed. For many classes of dye in aqueous solution, the band of highest intensity in dilute solution becomes weaker as the concentration is increased

and new bands appear at other wavelengths. These spectral changes have been attributed to aggregation of the dye molecules in water to form dimers and higher polymers, under the influence of the strong dispersion forces associated with the high polarisability of the chromophoric chain (21).

The dominant role of water as the solvent most favourable to aggregation at room temperature, is no doubt associated with the effect of its high dielectric constant in reducing the repulsive force, between the similarly charged dye cations or anions in the aggregate. The absence of aggregation in organic solvents of high dielectric constant (for example, ethanol) at room temperature (22), suggests that solvation interferes with the aggregation, and in such solvents, aggregates are stable only at low temperatures under conditions of high viscosity.

It has been found (23) that when aqueous tetramethylrhodamine isothiocyanate (TRITC) solutions are stored, the peak absorbance at 547 nm gives way to an absorption maximum of 499 nm, with a minor peak at 555 nm, and we may ascribe this to the formation of the dimer of tetramethylrhodamine.

Investigations were undertaken in order to ascertain the effect of detergent (sodium dodecyl sulphate) on the formation of tetramethylrhodamine, and fluorescein, dimers.

7.2.1. Fluorescent Modification of Proteins Utilising TRITC and Fluorescein Isothiocyanate (FITC).

Concentration ratios of TRITC dye to protein of 10-40 μg dye/mg protein, were regarded as optimal for efficient conjugation (24). A second report (25) has advocated 5 μg dye/

mg protein, as being the best dye : protein ratio. Similar dye : protein ratios were assumed for FITC.

As a consequence, a series of dye concentrations were utilised, ranging from 125 µg dye/mg protein to 0.2 µg dye/mg protein.

7.2.1.1. Experimental Procedure.

TRITC (0.6273 mg; 1.42 µmol) was dissolved in dimethylsulphoxide (DMSO, 0.502 ml), producing Solution A.

An aliquot (100 µl) of Solution A was taken and introduced into a tube. DMSO (400 µl) was added to this solution (Solution B).

An aliquot (100 µl) of Solution B was taken and introduced into a tube. DMSO (400 µl) was added to this solution (Solution C).

An aliquot (100 µl) of Solution C was taken and introduced into a tube. DMSO (400 µl) was added to this solution (Solution D).

An aliquot (100 µl) of Solution D was taken and introduced into a tube. DMSO (400 µl) was added to this solution (Solution E).

An aliquot (100 µl) of Solution E was taken and introduced into a tube. DMSO (400 µl) was added to this solution (Solution F).

Rabbit anti-Goat Immunoglobulin G (anti-GIgG, 16.2818 mg) was dissolved in carbonate buffer (0.05 M, 14.65 ml, pH 9.7).

Goat anti-Rabbit Immunoglobulin G (anti-RIgG, 16.0100 mg) was dissolved in carbonate buffer (0.05 M, 14.40 ml, pH 9.7).

Chicken Egg-White Lysozyme (Lysozyme, 8.0025 mg) was dissolved in carbonate buffer (0.05 M, 7.20 ml, pH 9.7).

Aliquots (4 x 80 µl) of Solution A were taken and each aliquot was placed into a separate tube, (100 µg per aliquot). This process was repeated for each Solution (up to Solution E).

Solution B contains 20.00 μg TRITC per aliquot.

Solution C contains 4.00 μg TRITC per aliquot.

Solution D contains 0.80 μg TRITC per aliquot.

Solution E contains 0.16 μg TRITC per aliquot.

Solution F contains 0.032 μg TRITC per aliquot.

Aliquots (80 μl) of Solution F were placed into each of two tubes.

An aliquot (720 μl) of stock aqueous anti-GIgG, was added to one tube of each solution set, (except Solution F).

An aliquot (720 μl) of stock aqueous anti-RIgG, was added to one tube of each solution set, (except Solution F).

An aliquot (720 μl) of stock aqueous lysozyme, was added to one tube of each solution set, (including Solution F).

An aliquot (720 μl) of the above carbonate buffer (0.05 M) was added to one tube of each solution set, (including Solution F).

FITC (0.6464 mg; 1.66 μmol) was dissolved in DMSO (0.517 ml), producing Solution G.

An aliquot (100 μl) of Solution G was taken and introduced into a tube. DMSO (400 μl) was added to this solution (Solution H).

An aliquot (100 μl) of Solution H was taken and introduced into a tube. DMSO (400 μl) was added to this solution (Solution I).

An aliquot (100 μl) of Solution I was taken and introduced into a tube. DMSO (400 μl) was added to this solution (Solution J).

An aliquot (100 μl) of Solution J was taken and introduced into a tube. DMSO (400 μl) was added to this solution (Solution K).

Aliquots (3 x 80 μl) of Solution G were taken and each aliquot was placed into a separate tube, (100 μg per aliquot).

This process was repeated for each Solution.

Solution H contains 20.00 μg FITC per aliquot.

Solution I contains 4.00 μg FITC per aliquot.

Solution J contains 0.80 μg FITC per aliquot.

Solution K contains 0.16 μg FITC per aliquot.

An aliquot (720 μl) of stock aqueous anti-GIgG, was added to one tube of each solution set.

An aliquot (720 μl) of stock aqueous anti-RIgG, was added to one tube of each solution set.

An aliquot (720 μl) of the above carbonate buffer (0.05 M) was added to one tube of each solution set.

Each preparation was allowed to stand overnight at 4°C. Each protein-containing preparation was then dialysed extensively (3 days) against phosphate buffered saline (0.10 M, 600 ml, pH 7.4), using cellulose tubing which retains molecular weight species in excess of 12000 daltons.

Portions (10 μl) of these preparations were taken and absorption spectra, were then undertaken. Aqueous sodium dodecyl sulphate (40 μl , 20% w/v), was added to the remainder of each preparation, producing a final concentration of 1% v/v sodium dodecyl sulphate (SDS). These preparations were allowed to incubate at room temperature for one hour.

Portions (10 μl) were then taken from each preparation, and absorption spectra were then undertaken.

7.2.1.2. Results for Free TRITC and its Protein Conjugates
Both in the Presence and Absence of SDS.

TRITC conc.	Absorption Wavelength			
	280 nm	499 nm	520 nm	547 nm
125 µg/mg protein	0.0045	0.0029	0.0042	0.0031
25 µg/mg protein	0.0065	0.0009	0.0016	0.0016
5 µg/mg protein	0.0062	0.0003	0.0004	0.0005

Table 7.1. Absorbance readings
of TRITC/anti-GIgG Conjugate.

TRITC conc.	Absorption Wavelength			
	280 nm	499 nm	520 nm	547 nm
125 µg/mg protein	0.0104	0.0022	0.0042	0.0091
25 µg/mg protein	0.0070	0.0006	0.0013	0.0030
5 µg/mg protein	0.0060	0.0001	0.0002	0.0004

Table 7.2. Absorbance readings
of TRITC/anti-GIgG Conjugate plus SDS.

TRITC conc.	Absorption Wavelength			
	280 nm	499 nm	520 nm	547 nm
125 µg/mg protein	0.0050	0.0040	0.0070	0.0040
25 µg/mg protein	0.0068	0.0009	0.0018	0.0015
5 µg/mg protein	0.0066	0.0004	0.0005	0.0005

Table 7.3. Absorbance readings
of TRITC/anti-RIgG Conjugate.

TRITC conc.	Absorption Wavelength			
	280 nm	499 nm	520 nm	547 nm
125 µg/mg protein	0.0118	0.0030	0.0059	0.0136
25 µg/mg protein	0.0106	0.0010	0.0018	0.0040
5 µg/ml protein	0.0082	0.0007	0.0007	0.0009

Table 7.4. Absorbance readings
of TRITC/anti-RIgG Conjugate plus SDS.

TRITC conc.	Absorption Wavelength			
	280 nm	499 nm	520 nm	547 nm
125 µg/mg protein	0.0090	0.0090	0.0070	0.0110
25 µg/mg protein	0.0060	0.0010	0.0010	0.0050
5 µg/mg protein	0.0160	0.0010	0.0010	0.0020
1 µg/mg protein	0.0250	0.0030	0.0020	0.0010
0.2 µg/mg protein	0.0410	0.0050	0.0040	0.0020
0.04 µg/mg protein	0.0260	0.0020	0.0020	0.0010

Table 7.5. Absorbance readings of TRITC/Lysozyme Conjugate.

TRITC conc.	Absorption Wavelength			
	280 nm	499 nm	520 nm	547 nm
125 µg/mg protein	0.0800	0.0080	0.0160	0.0280
25 µg/mg protein	0.0560	0.0040	0.0040	0.0080

Table 7.6. Absorbance readings of TRITC/Lysozyme Conjugate plus SDS.

TRITC conc.	Absorption Wavelength		
	499 nm	520 nm	547 nm
125 µg/ml	0.1360	0.0550	0.0430
25 µg/ml	0.0180	0.0165	0.0300
5 µg/ml	0.0026	0.0038	0.0080

Table 7.7. Absorbance readings of Free TRITC.

TRITC conc.	Absorption Wavelength		
	499 nm	520 nm	547 nm
125 µg/ml	0.0480	0.0870	0.1830
25 µg/ml	0.0090	0.0180	0.0450
5 µg/ml	0.0019	0.0034	0.0090

Table 7.8. Absorbance readings of Free TRITC plus SDS.

7.2.1.3. Results for Free FITC and its Protein Conjugates
Both in the Presence and Absence of SDS.

FITC conc.	Absorption Wavelength	
	280 nm	491 nm
125 µg/mg protein	0.0099	0.0060
25 µg/mg protein	0.0074	0.0020
5 µg/mg protein	0.0061	0.0003

Table 7.9. Absorbance readings
of FITC/anti-GIgG Conjugate.

FITC conc.	Absorption Wavelength	
	280 nm	491 nm
125 µg/mg protein	0.0104	0.0037
25 µg/mg protein	0.0085	0.0013
5 µg/mg protein	0.0075	0.0003

Table 7.10. Absorbance readings
of FITC/anti-GIgG Conjugate plus SDS.

FITC conc.	Absorption Wavelength	
	280 nm	491 nm
125 µg/mg protein	0.0104	0.0068
25 µg/mg protein	0.0074	0.0024
5 µg/mg protein	0.0067	0.0004

Table 7.11. Absorbance readings
of FITC/anti-RIgG Conjugate.

FITC conc.	Absorption Wavelength	
	280 nm	491 nm
125 µg/mg protein	0.0112	0.0037
25 µg/mg protein	0.0093	0.0016
5 µg/mg protein	0.0077	0.0004

Table 7.12. Absorbance readings
of FITC/anti-RIgG Conjugate plus SDS.

	Absorption Wavelength
FITC conc.	491 nm
125 µg/ml	0.1120
25 µg/ml	0.0250
5 µg/ml	0.0055

Table 7.13. Absorbance readings of Free FITC.

	Absorption Wavelength
FITC conc.	491 nm
125 µg/ml	0.0690
25 µg/ml	0.0180
5 µg/ml	0.0051

Table 7.14. Absorbance readings of Free FITC plus SDS.

7.2.1.4. Summary of Results.

The visible absorption spectrum of free TRITC exhibits a two peak spectrum, showing a major peak at 547 nm, and a minor peak at approximately 520 nm. On conjugation to protein, the TRITC molecule shows a two peak spectrum characterised by a major peak at 520 nm, and a minor peak at 547 nm.

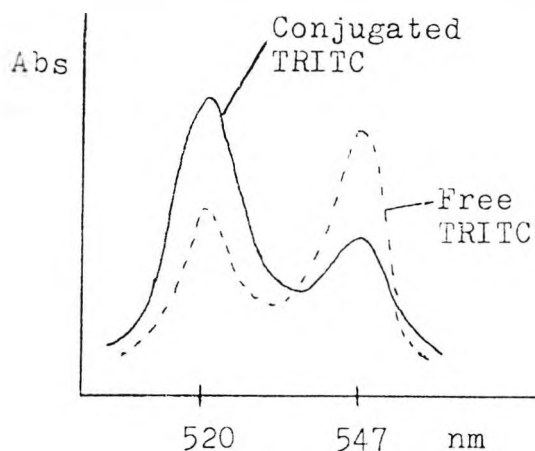


Fig. 7.5. Presentation of the visible spectrum of Free- and Conjugated TRITC.

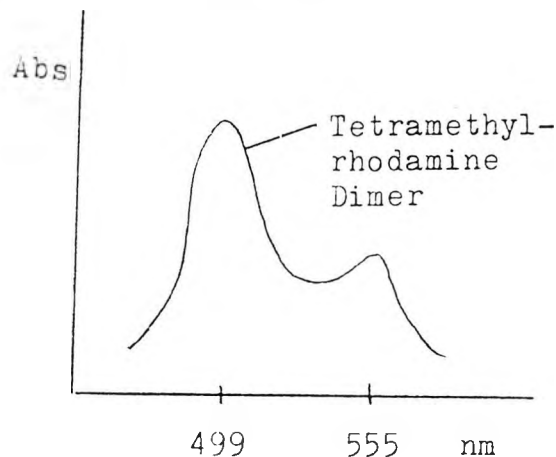


Fig. 7.6. Presentation of the visible spectrum of the tetramethyl-rhodamine dimer.

For free TRITC in aqueous buffered solution, pH 7.4 at a concentration of 125 $\mu\text{g}/\text{ml}$, the absorbance peak at 499 nm, (that is, absorption of the rhodamine dimer) is approximately three times that at 547 nm. At lower levels of TRITC, the absorbance peak at 547 nm is the dominant feature.

It is reasonable to assume that aggregation is more likely to occur at higher dye concentrations, and this may explain why the peak at 547 nm, (which is associated with the monomer) is more prominent at lower levels of TRITC.

Addition of SDS to the free TRITC preparation at a concentration of 125 $\mu\text{g}/\text{ml}$, causes the peak at 499 nm to diminish by approximately 183% with a concomitant increase, by approximately 340%, in the absorbance at 547 nm. Addition of SDS to the preparation containing lower levels of free TRITC, showed minimal changes in the absorbances at these wavelengths.

Similarly, for TRITC labelled anti-GIgG with the former present at an original concentration of 125 $\mu\text{g}/\text{mg}$ protein, when treated with SDS, the peak absorbance at 499 nm was observed to decrease by approximately 24% with a concomitant increase of 193% in the absorbance maximum at 547 nm. Addition of SDS to the preparations containing lower levels of TRITC showed minimal changes in the absorbance at these wavelengths.

The TRITC/anti-RIgG and the TRITC/Lysozyme conjugates, with the TRITC present at the highest concentration, exhibited similar trends, although the latter to a lesser extent.

In contrast, free FITC in aqueous buffered solution pH 7.4, exhibits an absorption maximum at 491 nm, which is attributed

to the monomer (26). Addition of SDS to a solution of FITC containing 125 $\mu\text{g/ml}$, gave rise to a decrease in absorbance at 491 nm of approximately 38%. Preparations containing lower levels of FITC showed minimal decreases in absorbance at 491 nm when treated with SDS.

Similarly, for FITC labelled anti-G1gG with the former present at an original concentration of 125 $\mu\text{g/ml}$ when treated with SDS, the peak absorbance at 491 nm was observed to decrease by approximately 38%. Again, a minimal decrease in absorbance at 491 nm was observed for the preparations containing lower levels of FITC, when treated similarly.

The FITC/anti-R1gG conjugate exhibited a similar trend. These data imply that the higher aggregates of at least TRITC are also formed in the presence of the corresponding protein-probe conjugate.

The absorption spectra obtained in the absence of SDS for the TRITC/protein conjugates, allows the deduction of the stoichiometry of the labelling.

7.2.1.5. Stoichiometry of Labelling.

A concentration ratio of 25 $\mu\text{g dye/mg protein}$ was utilised in the calculation, since this was regarded as the optimal ratio in order to avoid non-specific labelling. The protein concentration of the conjugates was determined utilising a documented formula (27).

$$\text{protein (mg/ml)} = \frac{0.D._{280 \text{ nm}} - (0.56 \times 0.D._{520 \text{ nm}})}{1.4}$$

This protein concentration was then used to deduce the stoichiometry of labelling (28).

$$\mu\text{M TRITC}/\mu\text{M protein} = \frac{\text{O.D.}_{547 \text{ nm}}}{\text{protein conc. mg/ml}} \times 6.6$$

where the value 6.6 represents the ratio between 0.041 (the factor to obtain the number of μM TRITC from the absorbance at 547 nm), and 0.00625 (the factor to transform the protein concentration in mg into μM of IgG).

7.2.1.6. Calculation of the Stoichiometry of Labelling for TRITC/anti-IgG Conjugate.

$$\text{protein (mg/ml)} = \frac{0.0065 - (0.56 \times 0.0016)}{1.4} = 4 \times 10^{-3} \text{ mg/ml}$$

$$\frac{0.0016}{4 \times 10^{-3}} \times 6.6 = \underline{2.64}$$

Therefore, the dye : protein ratio may be taken as 3 : 1.

Lysozyme, obtained from chicken egg-white, is composed of 129 amino acids of which six are lysine residues (29), but only one is available for fluorescent modification, via the ϵ -amino group (30). This residue was later found to be lysine-33 (31).

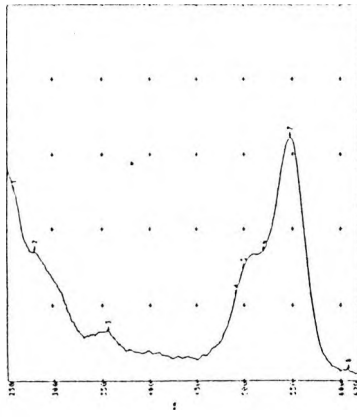


Fig. 7.7. U.V./visible spectrum of Free TRITC at a concentration of 5 µg/ml.

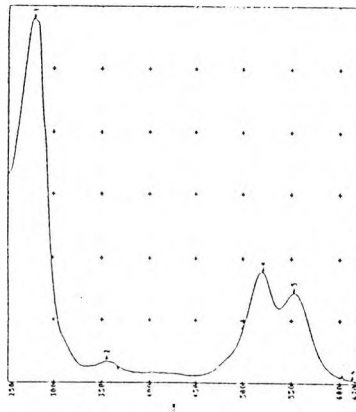


Fig. 7.8. U.V./visible spectrum of the TRITC/anti-GIgG Conjugate.

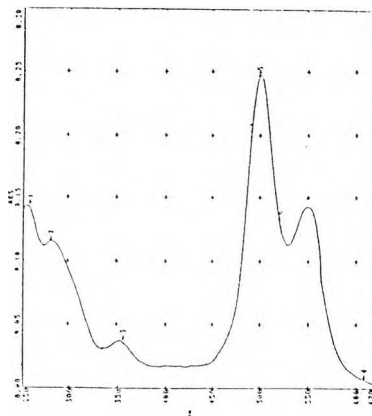


Fig. 7.9. U.V./visible spectrum of Free TRITC at a concentration of 125 µg/ml.

7.2.2. Effect of Removal of SDS from the TRITC-Protein Conjugates.

7.2.2.1. Experimental Procedure.

The TRITC-protein conjugates were prepared as previously described, in Section 7.2.1.1., using concentrations of TRITC at 125 µg/ml. Aqueous SDS (40 µl, 20% w/v) was added to each preparation, producing a final concentration of 1% v/v SDS. The absorbances at 499 nm, 520 nm and 547 nm were then recorded.

These preparations were then dialysed extensively (3 days) against PBS (0.10 M, 600 ml, pH 7.4). The absorbances at these wavelengths were then re-recorded.

7.2.2.2. Results.

TRITC conc.	Absorption Wavelength			
	280 nm	499 nm	520 nm	547 nm
125 µg/mg protein	0.0150	0.0070	0.0130	0.0240

Table 7.15. Absorbance readings of TRITC/anti-GIgG Conjugate plus SDS.

TRITC conc.	Absorption Wavelength			
	280 nm	499 nm	520 nm	547 nm
125 µg/mg protein	0.0104	0.0174	0.0194	0.0177

Table 7.16. Absorbance readings of TRITC/anti-GIgG Conjugate after Dialysis.

TRITC conc.	Absorption Wavelength			
	280 nm	499 nm	520 nm	547 nm
125 µg/mg protein	0.0200	0.0090	0.0200	0.0460

Table 7.17. Absorbance readings of TRITC/Lysozyme Conjugate plus SDS.

TRITC conc.	Absorption Wavelength			
	280 nm	499 nm	520 nm	547 nm
125 µg/mg protein	0.0180	0.0110	0.0265	0.0186

Table 7.18. Absorbance readings of TRITC/Lysozyme Conjugate after Dialysis.

7.2.2.3. Summary of Results.

The U.V./visible spectrum of the TRITC/anti-G1gG and the TRITC/Lysozyme conjugates, both at a dye concentration of 125 µg/mg protein in the presence of SDS, shows that the dominant peak occurs at 547 nm, with a minor peak at 499 nm.

It may be seen from the results, that removal of SDS via dialysis, brought about an increase, in the peak absorbance at 499 nm, of approximately 149% together with a decrease, in the peak at 547 nm, of approximately 27%.

Similar treatment of the TRITC/Lysozyme preparation, at a dye concentration of 125 µg/mg protein, showed an increase of approximately 23% in the 499 nm peak, concomitant with a decrease of approximately 60% in the peak at 547 nm.

These results indicate that the effect of SDS may be reversed by the subsequent removal of SDS. It may be deduced that the SDS serves to inhibit formation of rhodamine dimers.

7.2.3. Investigation of the Action of Urea, 2-Mercaptoethanol and SDS on Commercial TRITC-Protein Conjugates.

7.2.3.1. Experimental Procedure.

TRITC/Human Polyvalent Immunoglobulins (IgG, IgA, IgM), TRITC/Human IgG and TRITC/anti-G1gG conjugates, were obtained. These were designated T8, T9 and T10 respectively, and were subjected to various manipulations.

The commercial conjugates were subjected to U.V./visible spectral analysis. They were then treated with a mixture of aqueous urea (8 M) and 2-mercaptoethanol (40 μ l), producing a final concentration of 5% v/v. The conjugates were then incubated with SDS (60 μ l, 20% w/v), producing a final SDS concentration of 1% v/v. Absorption spectra were recorded subsequent to each treatment.

7.2.3.2. Results.

Treatment	Absorption Wavelength			
	280 nm	499 nm	520 nm	547 nm
0.10 M PBS	0.310	0.021	0.044	0.048
plus 8 M Urea and 5% v/v 2-mercaptoethanol	0.315	0.016	0.041	0.065
plus 1% v/v SDS	0.342	0.017	0.037	0.086

Table 7.19. Absorbance readings
of Conjugate T8.

Treatment	Absorption Wavelength			
	280 nm	499 nm	520 nm	547 nm
0.10 M PBS	0.338	0.047	0.105	0.085
plus 8 M Urea and 5% v/v 2-mercaptoethanol	0.354	0.037	0.099	0.125
plus 1% v/v SDS	0.373	0.036	0.076	0.182

Table 7.20. Absorbance readings
of Conjugate T9.

Treatment	Absorption Wavelength			
	280 nm	499 nm	520 nm	547 nm
0.10 M PBS	0.199	0.015	0.035	0.032
plus 8 M Urea and 5% v/v 2-mercaptoethanol	0.198	0.012	0.035	0.048
plus 1% v/v SDS	0.212	0.012	0.026	0.064

Table. 7.21. Absorbance readings
of Conjugate T10.

7.2.3.3. Stoichiometry of Labelling of the Commercial Conjugates.

For Conjugate T8.

$$\text{protein (mg/ml)} = \frac{0.310 - (0.56 \times 0.044)}{1.4} = 0.20 \text{ mg/ml}$$

$$\mu\text{M TRITC}/\mu\text{M protein} = \frac{0.048}{0.20} \times 6.6 = \underline{1.58}$$

Therefore, the dye : protein ratio for Conjugate T8 is taken as 2 : 1.

For Conjugate T9.

$$\text{protein (mg/ml)} = \frac{0.338 - (0.56 \times 0.105)}{1.4} = 0.199 \text{ mg/ml}$$

$$\mu\text{M TRITC}/\mu\text{M protein} = \frac{0.085}{0.199} \times 6.6 = \underline{2.80}$$

Therefore, the dye : protein ratio for Conjugate T9 is taken as 3 : 1.

For Conjugate T10

$$\text{protein (mg/ml)} = \frac{0.199 - (0.56 \times 0.035)}{1.4} = 0.128 \text{ mg/ml}$$

$$\mu\text{M TRITC}/\mu\text{M protein} = \frac{0.032}{0.128} \times 6.6 = \underline{1.65}$$

Therefore, the dye : protein ratio for Conjugate T10 is taken as 2 : 1.

7.2.3.4. Summary of Results.

Addition of the urea/2-mercaptoethanol mixture to the

conjugate T9, produced an approximate decrease in absorbance at 499 nm, (that is, due to the dimer), of 21% together with an increase in absorbance of 47%, at 547 nm. Addition of SDS, produced a further decrease of approximately 3% in the absorbance at 499 nm, concomitant with a further increase in absorbance at 547 nm, of approximately 46%. This pattern of behaviour was repeated for conjugates T8 and T10.

We may conclude, therefore, that the urea/2-mercapto-ethanol mixture prevents dimerisation of rhodamine to a degree, but dimer formation may be further disrupted by the addition of SDS.

7.2.4. Investigation of the Interaction Between Free TRITC & Free FITC as well as Their Protein Conjugates and SDS, as Detected by Fluorescence Spectroscopy.

7.2.4.1. Experimental Procedure for the Fluorescent Modification of Proteins Utilising TRITC & FITC.

Three proteins (anti-GIgG, anti-RIgG and Lysozyme), were fluorescently modified with TRITC as previously described in Section 7.2.1.1. A series of TRITC solutions were prepared at various concentrations.

Anti-GIgG and anti-RIgG were fluorescently modified with FITC, as previously described in Section 7.2.1.1. A series of FITC solutions were prepared at various concentrations.

These solutions were then subjected to fluorescence spectral analysis. The fluorescence spectrum of free TRITC exhibits a peak emission at 580 nm on excitation.

7.2.4.2. Results for Free TRITC and its Protein Conjugates.

Fluorescence Emission at 580 nm.

R.F.I. = Relative Fluorescence Intensity.

TRITC conc.	R.F.I. at Excitation Wavelength		
	499 nm	520 nm	547 nm
125 µg/mg protein	9.00	14.50	33.00
25 µg/mg protein	7.50	12.00	28.00
5 µg/mg protein	1.67	2.40	6.20

Table 7.22. R.F.I. readings of TRITC/anti-GIgG Conjugate.

TRITC conc.	R.F.I. at Excitation Wavelength		
	499 nm	520 nm	547 nm
125 µg/mg protein	27.50	60.00	138.00
25 µg/mg protein	10.00	18.00	44.00
5 µg/mg protein	2.40	4.00	10.50

Table 7.23. R.F.I. readings of TRITC/anti-GIgG Conjugate plus SDS.

TRITC conc.	R.F.I. at Excitation Wavelength		
	499 nm	520 nm	547 nm
125 µg/mg protein	8.00	13.00	29.00
25 µg/mg protein	7.00	10.20	24.00
5 µg/mg protein	1.50	2.40	5.10

Table 7.24. R.F.I. readings of TRITC/anti-RIgG Conjugate.

TRITC conc.	R.F.I. at Excitation Wavelength		
	499 nm	520 nm	547 nm
125 µg/mg protein	25.50	45.00	100.00
25 µg/mg protein	9.00	15.00	38.00
5 µg/mg protein	2.20	3.60	8.60

Table 7.25. R.F.I. readings of TRITC/anti-RIgG Conjugate plus SDS.

TRITC conc.	R.F.I. at Excitation Wavelength		
	499 nm	520 nm	547 nm
125 µg/mg protein	7.90	13.00	29.40
25 µg/mg protein	6.70	10.30	24.20
5 µg/mg protein	1.50	2.30	5.50
1 µg/mg protein	0.20	0.50	1.10

Table 7.26. R.F.I. readings of TRITC/Lysozyme Conjugate.

TRITC conc.	R.F.I. at Excitation Wavelength		
	499 nm	520 nm	547 nm
125 µg/mg protein	24.00	49.00	98.00
25 µg/mg protein	9.00	15.00	35.00
5 µg/mg protein			8.90
1 µg/mg protein			1.80

Table 7.27. R.F.I. readings of TRITC/Lysozyme Conjugate plus SDS.

TRITC conc.	R.F.I. at Excitation Wavelength	
	499 nm	547 nm
125 µg/ml	26.00	102.00
25 µg/ml	18.00	68.00
5 µg/ml	9.20	33.00
1 µg/ml	1.96	6.90
0.2 µg/ml	0.55	2.02
0.04 µg/ml	0.11	0.37

Table 7.28. R.F.I. readings of Free TRITC.

	R.F.I. at Excitation Wavelength
TRITC conc.	547 nm
125 µg/ml	1410.00
25 µg/ml	333.00
5 µg/ml	58.50
1 µg/ml	11.60
0.2 µg/ml	2.96
0.04 µg/ml	0.66

Table 7.29. R.F.I. readings
of Free TRITC plus SDS.

7.2.4.3. Results for Free FITC and its Protein Conjugates.

Fluorescence Emission at 515 nm.

	R.F.I. at Excitation Wavelength
FITC conc.	491 nm
125 µg/mg protein	78.100
25 µg/mg protein	36.300
5 µg/mg protein	3.420
1 µg/mg protein	0.820
0.2 µg/mg protein	0.252

Table 7.30. R.F.I. readings
of FITC/anti-GIgG Conjugate.

	R.F.I. at Excitation Wavelength
FITC conc.	491 nm
125 µg/mg protein	36.000
25 µg/mg protein	14.700
5 µg/mg protein	2.000
1 µg/mg protein	0.600
0.2 µg/mg protein	0.300

Table 7.31. R.F.I. readings
of FITC/anti-GIgG Conjugate plus SDS.

FITC conc.	R.F.I. at Excitation Wavelength 491 nm
125 µg/mg protein	61.600
25 µg/mg protein	39.100
5 µg/mg protein	3.840
1 µg/mg protein	1.180
0.2 µg/mg protein	0.354

Table 7.32. R.F.I. readings
of FITC/anti-R1gG Conjugate.

FITC conc.	R.F.I. at Excitation Wavelength 491 nm
125 µg/mg protein	20.600
25 µg/mg protein	10.700
5 µg/mg protein	1.240
1 µg/mg protein	0.600
0.2 µg/mg protein	0.350

Table 7.33. R.F.I. readings
of FITC/anti-R1gG Conjugate plus SDS.

FITC conc.	R.F.I. at Excitation Wavelength 491 nm
125 µg/ml	381.00
25 µg/ml	187.50
5 µg/ml	52.50
1 µg/ml	8.60
0.2 µg/ml	2.07

Table 7.34. R.F.I. readings
of Free FITC.

	R.F.I. at Excitation Wavelength
FITC conc.	491 nm
125 µg/ml	243.00
25 µg/ml	130.00
5 µg/ml	35.00
1 µg/ml	6.60
0.2 µg/ml	1.90

Table 7.35. R.F.I. readings
of Free FITC plus SDS.

7.2.4.4. Summary of Results.

For free TRITC in aqueous buffered solution (pH 7.4), at a concentration of 125 µg/ml, the relative fluorescence intensity at 580 nm, when excited at 547 nm, was found to be approximately twelve-times that observed on excitation at 499 nm (at constant absorbance of 0.08 at the respective excitation wavelengths). Less dramatic results were found for lower levels of TRITC. Addition of SDS, caused the emission peak at 580 nm (on excitation at 547 nm), to increase almost fourteen-fold over the emission observed in the absence of SDS. Again, less dramatic results were observed for lower levels of TRITC. Similarly, for TRITC labelled anti-GIgG, with the former present at an original concentration of 125 µg/ml, the relative fluorescence intensity at 580 nm, when excited at 547 nm, was found to be almost four-times that observed on excitation at 499 nm (at constant absorbance of 0.07 at the respective excitation wavelength). The lower levels of TRITC originally present, exhibited minimal increases in the relative fluorescence intensity at 580 nm, when excited

at 547 nm than when excited at 499 nm.

Addition of SDS produced an emission peak at 580 nm (on excitation at 547 nm) over four-times more intense than that observed in the absence of SDS. Again, less dramatic results were obtained for lower levels of TRITC, and similar results were obtained for TRITC-modified anti-RIGG as well as TRITC-modified Lysozyme.

In contrast, free FITC in aqueous buffered solution (pH 7.4) exhibits a fluorescence spectrum, with peak emission at 515 nm when excited at 491 nm. Addition of SDS to the preparation containing 125 $\mu\text{g/ml}$ FITC, produced a decrease in the relative fluorescence intensity at 515 nm, when excited at 491 nm, of approximately 39%. Less dramatic results were obtained for lower levels of FITC. Similarly, for FITC labelled anti-GIGG, with the former present at an original concentration of 125 $\mu\text{g/ml}$, the relative fluorescence intensity at 515 nm (excitation at 491 nm), in the presence of SDS was found to be decreased by approximately 54%, when compared to the relative fluorescence intensity in the absence of SDS.

Lower original levels of FITC, exhibited less dramatic changes in the relative fluorescence intensity. Similar treatment for anti-RIGG with the former present at an original concentration of 125 $\mu\text{g/ml}$, yielded a decrease in the relative fluorescence intensity, on SDS addition, of almost 67% as compared to the emission in the absence of SDS. Again, lower original levels of FITC exhibited less dramatic changes in the relative fluorescence intensity on SDS addition.

7.2.4.5. Conclusion.

In the case of TRITC, it is possible that two TRITC molecules may interact when they are in close proximity to each other, by the native conformation of the protein. This dimer could give rise to the dominant peak at 499 nm. Addition of aqueous urea (8 M), unwinds the protein such that it is only stabilised by the presence of disulphide linkages between cysteine residues. 2-mercaptoethanol (5% v/v) was added in order to reduce these disulphide bridges, so that the protein is now devoid of its higher structure. The protein is now present as long polypeptide strands, and the unwinding action of urea and 2-mercaptoethanol may pull apart the TRITC molecules present on distant regions of the protein. Thus, an increase in absorbance at 547 nm was observed, which is attributable to the TRITC monomer.

However, this hypothesis does not explain the finding that dimerisation of the free TRITC occurs in solution, and addition of SDS yields an increase in the peak absorbance attributable to the monomer. Moreover, the TRITC-Lysozyme conjugation medium also exhibited the presence of TRITC dimers, albeit to a lesser extent. Since lysozyme possesses just one site for binding, TRITC dimers in this case, may not be formed between two TRITC molecules on the same polypeptide chain. Thus, TRITC dimers must be formed between TRITC molecules present on different protein strands, provided no free TRITC is present.

SDS possesses a net negative charge; since the TRITC molecule possesses a positively charged nitrogen atom, it is

conceivable that an electrostatic attraction between the TRITC molecule and the SDS may occur. This would tend to destabilise aggregation, and would promote the dissociation of the dimer into monomers. This may explain the increase in the peak absorption of the monomer on SDS addition.

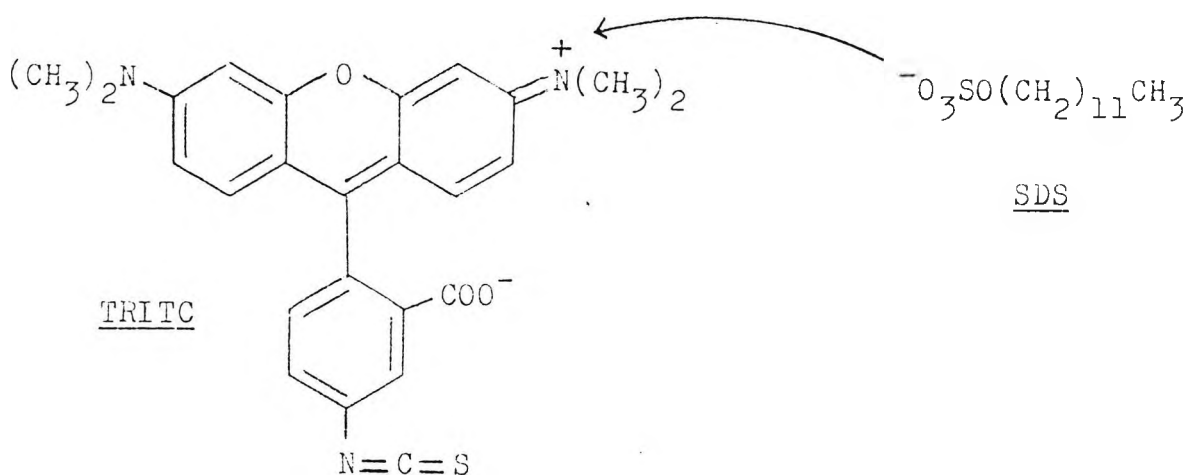


Fig. 7.10. The electrostatic interaction between TRITC and SDS destabilises aggregation.

It has been found (32), that anionic surfactants such as sodium lauryl sulphate, were more effective in the suppression of aggregate formation of rhodamine 6G, than neutral surfactants, such as Triton X-100. Cationic surfactants, such as cetyl triethyl ammonium bromide, were found to have no effect on the capacity of aggregation of the dye.

Thus, it may be envisaged that dimerisation of TRITC may occur in at least four different ways: between;

- i) TRITC molecules present on one protein molecule;
- ii) TRITC molecules present on different protein molecules;
- iii) Free TRITC molecules present in solution, and
- iv) a protein-bound TRITC molecule and a free TRITC molecule in solution. The greater levels of fluorescence emission

observed in the presence of SDS, are a consequence of the presence of higher levels of monomer under these conditions.

Conversely, for FITC in solution and when protein-bound, addition of SDS decreases the peak absorption at 491 nm attributable to the monomer. It is likely that addition of SDS promotes the formation of fluorescein micelles. Thus, the presence of SDS may promote aggregation of the fluorescein molecules and therefore a decrease in absorbance of the monomer, (at 491 nm), is observed.

This contention is supported by the finding that the absorption spectrum of FITC/anti-GIgG preparation containing 125 $\mu\text{g/ml}$ FITC, possesses the monomer peak at 491 nm. On addition of SDS, this absorption maximum gives way to a two-peak spectrum exhibiting maxima at approximately 463 nm and 480 nm. The peak at approximately 463 nm, is indicative of dimer formation (33).

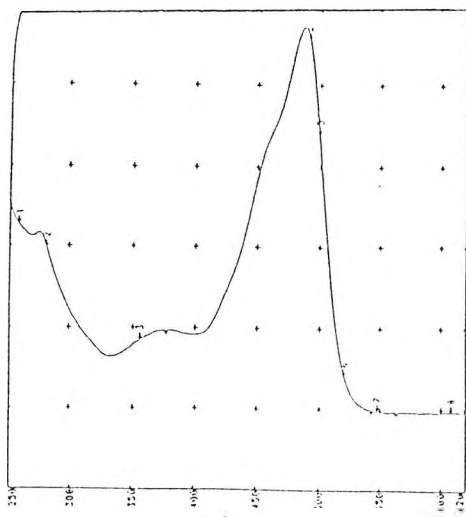


Fig. 7.11. U.V./visible spectrum of Free FITC.

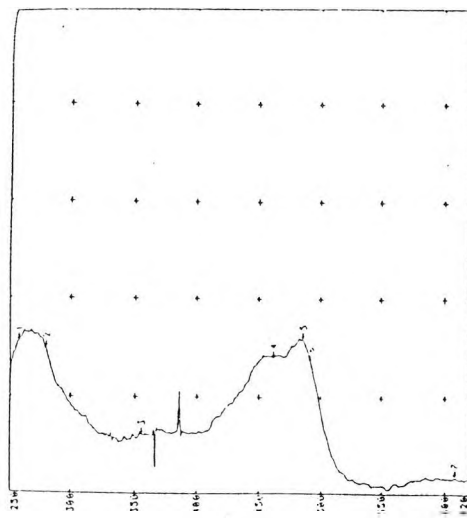


Fig. 7.12. U.V./visible spectrum of Free FITC in the presence of SDS.

7.3. FURTHER INVESTIGATIONS INTO THE SELF-ASSOCIATION PROCESS.

7.3.1. The Preparation of the TRITC/Glycine Conjugate.

Investigations were undertaken, via the interaction of TRITC with glycine, in order to further deduce the nature of the self-association process.

7.3.1.1. Experimental Procedure.

TRITC (0.6418 mg; 1.45 μ mol) was dissolved in dimethylsulphoxide (DMSO, 0.513 ml), producing Solution A.

An aliquot (100 μ l) of Solution A was taken and introduced into a tube. DMSO (400 μ l) was added to this solution (Solution B).

An aliquot (100 μ l) of Solution B was taken and introduced into a tube. DMSO (400 μ l) was added to this solution (Solution C).

Glycine (0.1389 mg; 1.85 μ mol) was dissolved in carbonate buffer (0.05 M, 1.60 ml, pH 9.7).

Aliquots (2 x 80 μ l) of Solution A were taken and each aliquot was placed into a separate tube, (100 μ g per aliquot). To one tube was added an aliquot (720 μ l) of the carbonate buffer. To the other tube was added glycine solution (720 μ l). (0.0625 mg glycine per aliquot)

This procedure was repeated with Solution C (5 μ g TRITC per aliquot), and the solutions were allowed to stand overnight at room temperature. Absorption spectra of the solutions were then undertaken.

7.3.1.2. Results.

TRITC conc.	Absorption Wavelength		
	499 nm	520 nm	547 nm
125 µg/ml	0.1210	0.0630	0.0690
5 µg/ml	0.0030	0.0034	0.0067

Table 7.36. Absorbance readings of Free TRITC in buffer pH 9.7.

TRITC conc.	Absorption Wavelength		
	499 nm	520 nm	547 nm
125 µg/ml	0.0930	0.0780	0.1300
5 µg/ml	0.0022	0.0033	0.0073

Table 7.37. Absorbance readings of TRITC/Glycine Conjugate.

7.3.1.3. Summary of Results.

It may be seen from the results that for the preparation devoid of glycine, at a TRITC concentration of 125 µg/ml, the absorption maximum at 499 nm was 75% greater than that at 547 nm. In contrast, for the preparation at the same dye concentration containing glycine, the absorption maximum at 499 nm is approximately 40% less than that at 547 nm. For both preparations at a dye concentration of 5 µg/ml, the 547 nm absorption peak was the dominant feature.

These results suggest that tetramethylrhodamine (TMR) may dimerise when present at high concentrations, and in the absence of glycine; and the presence of glycine prevents dimerisation. It is likely that the alkalinity of the medium allows the amine group of the glycine molecules to be present in the unprotonated form.

As a consequence, covalent reaction may occur between the amine group of the amino acid and the isothiocyanate group of TRITC, producing a thiourea linkage.

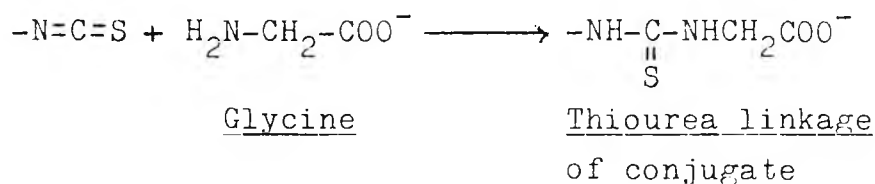


Fig. 7.13. Reaction between the isothiocyanate group of TRITC and glycine.

It is reasonable to suppose that glycine may prevent TMR dimerisation by disruption of the hydrogen bond formation, between TMR molecules which is thought to occur during dimerisation (33).

It is necessary for fluorophores to possess a reactive moiety so that they may conjugate with the particular species under investigation. TRITC is no exception, and the isothiocyanate group is susceptible to hydrolysis, producing a primary amine and acidic gases.



Fig. 7.14. Reaction for the hydrolysis of TRITC.

It is feasible for one TRITC molecule to be hydrolysed to a primary amine, and this may then react with a TRITC molecule that has not yet undergone hydrolysis. As a consequence, TRITC may self-associate covalently.

Aliquots (3 x 80 μ l) of Solution A were taken and each aliquot was placed into a separate tube, (100 μ g per aliquot). This process was repeated for each Solution.

Solution B contains 20.00 μ g fluorescein per aliquot.

Solution C contains 4.00 μ g fluorescein per aliquot.

Solution D contains 0.80 μ g fluorescein per aliquot.

Solution E contains 0.16 μ g fluorescein per aliquot.

An aliquot (720 μ l) of stock aqueous anti-GIgG, was added to one tube of each solution set.

An aliquot (720 μ l) of stock aqueous anti-RIgG, was added to one tube of each solution set.

An aliquot (720 μ l) of the above carbonate buffer (0.05 M) was added to one tube of each solution set.

All tubes were allowed to stand overnight at room temperature, protected from light. The preparations were then dialysed extensively (3 days) against phosphate buffered saline (0.10 M, 600 ml, pH 7.4).

The emission at 515 nm of the dialysand and dialysate of each preparation were then recorded.

7.3.2.2. Results.

Excitation Wavelength = 491 nm.

Fluorescein conc.	R.F.I. at Wavelength 515 nm	
	Dialysand	Dialysate
125 μ g/mg protein	1939.4	872700
25 μ g/mg protein	363.6	183660
5 μ g/mg protein	78.8	33660
1 μ g/mg protein	33.9	7080
0.2 μ g/mg protein	9.1	1620

Table 7.38. R.F.I. readings of
Fluorescein/anti-GIgG preparation.

Fluorescein conc.	R.F.I. at Wavelength 515 nm	
	Dialysand	Dialysate
125 µg/mg protein	1878.8	891000
25 µg/mg protein	351.5	176400
5 µg/mg protein	78.8	35460
1 µg/mg protein	46.1	8880
0.2 µg/mg protein	12.7	2100

Table 7.39. R.F.I. readings of
Fluorescein/anti-RiG preparation.

Fluorescein conc.	R.F.I. at Wavelength 515 nm	
	Dialysand	Dialysate
125 µg/ml	11.5	872680

Table 7.40. R.F.I. readings of
Fluorescein in the Absence of Protein.

7.3.2.3. Summary of Results.

For all fluorescein preparations in the presence of anti-GIgG, the percentage of fluorescein present in the dialysis subsequent to dialysis, as detected by emission at 515 nm on excitation at 491 nm, was found to be in the range of 0.20% to 0.56%. Similar results were obtained for fluorescein in the presence of anti-RIgG.

For fluorescein present at the highest concentration (125 µg/ml) in the absence of protein, only 0.001% was found in the dialysis sack after dialysis. This pattern was repeated for the lower levels of fluorescein utilised.

The results indicate that the level of fluorescein present in the dialysis sack when in conjunction with protein, is at least 200 times greater than that found in the absence of protein.

Since fluorescein may not covalently interact with the ϵ -amino groups of lysine residues present in the proteins, it would appear, therefore, that some non-specific binding of the fluorescein to the protein is occurring, and that the interaction of the dye with the protein, and with itself, is competing with any repulsive effects.

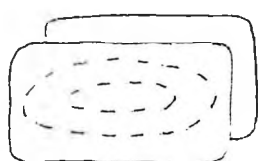
7.3.2.4. Conclusion.

It has been shown (34), that fluorescein molecules aggregate to produce a sandwich dimer, with a twist angle, θ , of 71° . Their interdipole distance was found to be 4.81 Å. Successive halogenation of the fluorescein molecules result in an increase in the interplanar distance, and consequently, there is observed a decrease in the angle θ between the transition dipoles.

Halo-substituted fluorescein aggregates containing four chlorine atoms and two iodine atoms, were found to possess a twist angle of 60° , together with an interplanar distance of 5.92 Å. The increased dipole strength due to substitution of more polarisable halogens, apparently creates a stronger field such that the dipoles tend toward parallel alignment. Better overlap due to more parallel geometry enhances the aggregation tendency, over-riding the steric effect. For twist angles of 60° , a 'sis-kebab' model of stacking (34) has been proposed, and the overall structure

would assume a helical conformation. This geometrical arrangement allows the trimer to be more stable than the dimer, and this hypothesis has been proposed for methylene blue aggregates (35).

Exciton theory (36) predicts that for parallel dimers (H-type), the absorption spectrum consists of a single-band blue-shifted with respect to the monomer. For head-to-tail dimers (J-type), the spectrum consists of a single-band red-shifted with respect to the monomer.



H-type
aggregate



J-type aggregate

Fig. 7.16. Presentation of the structures of H-type and J-type dye aggregates.

All xanthene dyes (37), of which rhodamines are an important group, produce dimers the structure of which, is of an intermediate geometry. In this case, band splitting is observed, (as seen by the formation of a major peak at 499 nm, with a minor peak at 555 nm).

It has been shown (38) that neutral rhodamine B exhibits dimers of intermediate structure.

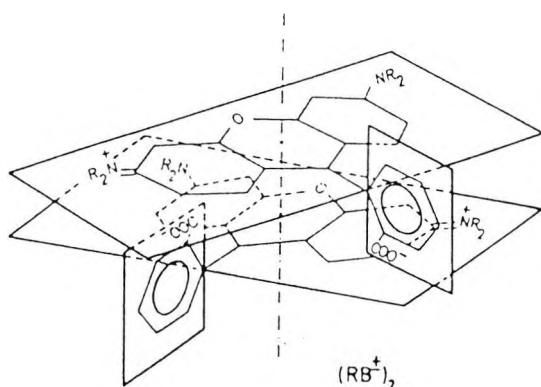


Fig. 7.17. Geometric structure of the neutral dimer of Rhodamine B (39).

The carboxyl groups of the monomers allows electrostatic interaction between the carboxyl group of a monomer, and a positively charged nitrogenated group of the other. This disposition reduces repulsive interaction, so that the aggregate is maximally stabilised.

The twist angle, θ , may be deduced from the relationship (34):

$$f_1/f_2 = \tan^2 (\theta/2)$$

where f_1 and f_2 are the absorption maxima for the long wavelength, and short wavelength peak respectively. From the spectrum as shown, the twist angle for the TRITC dimer may be determined.

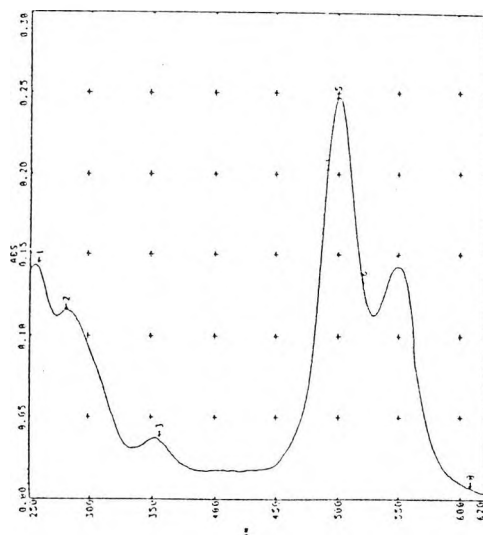


Fig. 7.18. U.V./visible spectrum of Free TRITC at a concentration of 125 µg/ml.

$$\frac{f_1 \text{ (peak at 555 nm)}}{f_2 \text{ (peak at 499 nm)}} = \frac{0.142}{0.245} = \underline{0.58}$$

$$0.58 = \tan^2 (\theta/2)$$

$$\underline{\theta = 75^\circ}$$

The calculated twist angle for the tetramethylrhodamine dimer, is slightly greater than that for the fluorescein dimer. This implies that the interdipole distance is shorter for tetramethylrhodamine, and this is to be expected given that the molecule possesses both a positive and a negative charge, and would thereby allow a more intimate association.

7.4. INVESTIGATION INTO THE PROCESS OF RESONANCE ENERGY TRANSFER FROM FLUORESCEIN TO TETRAMETHYL-RHODAMINE, AS ANALYSED BY ABSORPTION SPECTROSCOPY.

Since there exists an overlap in the absorption spectrum of TRITC, and the emission spectrum of FITC, it follows that excited state energy of FITC may be transferred to TRITC. Investigations were undertaken in order to deduce the nature of this phenomenon, via the production of Fluorescein/TMR dimers.

7.4.1. Experimental Procedure.

TRITC (0.1020 mg; 0.23 μmol) was dissolved in dimethylsulphoxide (DMSO, 0.204 ml), producing Solution A.

An aliquot (40 μl) of Solution A was taken and introduced into a tube. DMSO (160 μl) was added to this solution (Solution B).

An aliquot (40 μl) of Solution B was taken and introduced into a tube. DMSO (160 μl) was added to this solution (Solution C).

Aliquots (3 x 40 μl) of Solution A were taken and each aliquot was placed into a separate tube, (20 μg TRITC per aliquot). This process was repeated for each solution.

Solution B (4.0 μg TRITC per aliquot).

Solution C (0.8 μg TRITC per aliquot).

FITC (0.1057 mg; 0.27 μ mol) was dissolved in dimethylsulphoxide (DMSO, 0.211 ml) producing Solution D.

An aliquot (8 μ l, 4 μ g per aliquot) was added to each of the above tubes (total 9), together with DMSO (32 μ l).

An aliquot (720 μ l) of stock aqueous anti-GIgG, was added to one tube of each solution set.

An aliquot (720 μ l) of stock aqueous anti-RIgG, was added to one tube of each solution set.

An aliquot (720 μ l) of carbonate buffer (0.05 M, pH 9.7) was added to one tube of each solution set.

All tubes were allowed to stand overnight at room temperature, protected from light. The contents of each tube containing protein/dye, were transferred to a dialysis sack and dialysed extensively (3 days) against phosphate buffered saline (0.10 M, 600 ml, pH 7.4).

The samples were subjected to U.V./visible spectral analysis. SDS (40 μ l, 20% w/v), was added producing a final SDS concentration of 1% v/v. These samples were then re-subjected to U.V./visible spectral analysis.

7.4.2. Results.

TRITC conc. plus 5 μ g FITC/ mg protein.	Absorption Wavelength				
	280 nm	491 nm	499 nm	520 nm	547 nm
25 μ g/mg protein	0.0059	0.0009	0.0012	0.0018	0.0019
5 μ g/mg protein	0.0054	0.0005	0.0005	0.0003	0.0004
1 μ g/mg protein	0.0058	0.0004	0.0004	0.0001	0.0002

Table 7.41. Absorbance readings
of TRITC/FITC/anti-GIgG Conjugate.

TRITC conc. plus 5 µg FITC/ mg protein.	Absorption Wavelength				
	280 nm	491 nm	499 nm	520 nm	547 nm
25 µg/mg protein	0.0056	0.0006	0.0006	0.0100	0.0024
5 µg/mg protein	0.0061	0.0003	0.0003	0.0001	0.0003
1 µg/mg protein	0.0052	0.0001	0.0001	0.0001	0.0001

Table 7.42. Absorbance readings
of TRITC/FITC/anti-GIgG Conjugate plus SDS.

TRITC conc. plus 5 µg FITC/ mg protein.	Absorption Wavelength				
	280 nm	491 nm	499 nm	520 nm	547 nm
25 µg/mg protein	0.0057	0.0011	0.0014	0.0022	0.0019
5 µg/mg protein	0.0059	0.0007	0.0006	0.0003	0.0003
1 µg/mg protein	0.0074	0.0007	0.0006	0.0002	0.0003

Table 7.43. Absorbance readings
of TRITC/FITC/anti-RIgG Conjugate.

TRITC conc. plus 5 µg FITC/ mg protein.	Absorption Wavelength				
	280 nm	491 nm	499 nm	520 nm	547 nm
25 µg/mg protein	0.0066	0.0006	0.0006	0.0010	0.0023
5 µg/mg protein	0.0063	0.0004	0.0003	0.0003	0.0004
1 µg/mg protein	0.0054	0.0003	0.0001	0.0001	0.0002

Table 7.44. Absorbance readings
of TRITC/FITC/anti-RIgG Conjugate plus SDS.

TRITC conc. plus 5 µg FITC/ mg protein.	Absorption Wavelength			
	491 nm	499 nm	520 nm	547 nm
25 µg/mg protein	0.0230	0.0260	0.0220	0.0380
5 µg/mg protein	0.0080	0.0070	0.0050	0.0100
1 µg/mg protein	0.0090	0.0065	0.0020	0.0025

Table 7.45. Absorbance readings
of Free TRITC/Free FITC.

TRITC conc. plus 5 µg FITC/ mg protein.	Absorption Wavelength			
	491 nm	499 nm	520 nm	547 nm
25 µg/mg protein	0.0098	0.0112	0.0147	0.0343
5 µg/mg protein	0.0065	0.0058	0.0050	0.0104
1 µg/mg protein	0.0054	0.0040	0.0018	0.0029

Table 7.46. Absorbance readings
of Free TRITC/Free FITC plus SDS.

7.4.3. Summary of Results.

As expected for fluorescein, addition of SDS produced a decrease in absorbance at 491 nm in the presence of the highest concentration of TRITC, of approximately 57%. Decreases in absorbance of fluorescein were also observed in the presence of lower concentrations of TRITC. However, the expected sharp increase in the absorbance of TRITC at 547 nm, on addition of SDS, was not observed for any concentration of TRITC. Similar results were obtained for the TMR/Fluorescein-protein conjugates.

It is conceivable that the fluorescein molecule will absorb at 547 nm, and therefore excited state energy is transferred to the TMR from the fluorescein. As a consequence, the TMR molecule is excited indirectly and, the TMR already being in the excited state, will be unable to directly absorb exciting radiation from the external medium.

7.5. INVESTIGATION INTO THE FLUORESCENCE QUENCHING OF TETRAMETHYLRHODAMINE BY FLUORESCEIN, AS ANALYSED BY FLUORESCENCE SPECTROSCOPY.

If there is a degree of overlap between the emission

spectrum of one fluorescent molecule (donor), and the absorption spectrum of another molecule (acceptor), then it is possible for fluorescence of the donor to be quenched by the acceptor via energy transfer. In the case of fluorescein and TMR, the former has a peak emission at 515 nm, while the latter has a peak absorption at 547 nm. Since there is just 32 nm between these peaks, it follows that there should be a large overlap between the spectra.

Investigations were undertaken in order to deduce the nature of this phenomenon, via production of Fluorescein/TMR dimers.

7.5.1. Experimental Procedure.

The dimers were produced as previously described, in Section 7.4.1. The preparations obtained were then subjected to fluorescence spectral analysis.

7.5.2. Results.

TRITC conc. plus 5 µg FITC/ mg protein.	R.F.I. at Excitation Wavelength			
	491 nm	499 nm	520 nm	547 nm
25 µg/mg protein Emission at 515 nm	8.5			
Emission at 580 nm	7.0	8.7	12.9	29.1
5 µg/mg protein Emission at 515 nm	13.6			
Emission at 580 nm	3.2	3.3	3.7	8.5
1 µg/mg protein Emission at 515 nm	15.3			
Emission at 580 nm	2.0	1.6	0.8	1.7

Table 7.47. R.F.I. readings of
TRITC/FITC/anti-GIgG Conjugate.

TRITC conc. plus 5 µg FITC/ mg protein.	R.F.I. at Excitation Wavelength	
	491 nm	547 nm
25 µg/mg protein Emission at 515 nm Emission at 580 nm	3.90	150.0
5 µg/mg protein Emission at 515 nm Emission at 580 nm	4.80	12.6
1 µg/mg protein Emission at 515 nm Emission at 580 nm	4.80	3.0

Table 7.48. R.F.I. readings of
TRITC/FITC/anti-GIgG Conjugate plus SDS.

TRITC conc. plus 5 µg FITC/ mg protein.	R.F.I. at Excitation Wavelength			
	491 nm	499 nm	520 nm	547 nm
25 µg/mg protein Emission at 515 nm Emission at 580 nm	9.00 7.50	9.60	14.40	33.00
5 µg/mg protein Emission at 515 nm Emission at 580 nm	12.10 3.20	3.30	4.10	9.30
1 µg/mg protein Emission at 515 nm Emission at 580 nm	13.30 1.80	1.55	1.10	2.00

Table 7.49. R.F.I. readings of
TRITC/FITC/anti-RIGG Conjugate.

TRITC conc. plus 5 µg FITC/ mg protein.	R.F.I. at Excitation Wavelength	
	491 nm	547 nm
25 µg/mg protein Emission at 515 nm Emission at 580 nm	3.90	150.00
5 µg/mg protein Emission at 515 nm Emission at 580 nm	4.80	14.20
1 µg/mg protein Emission at 515 nm Emission at 580 nm	4.80	3.30

Table 7.50. R.F.I. readings of
TRITC/FITC/anti-R1gG Conjugate plus SDS.

TRITC conc. plus 5 µg FITC/ mg protein.	R.F.I. at Excitation Wavelength			
	491 nm	499 nm	520 nm	547 nm
25 µg/mg protein Emission at 515 nm Emission at 580 nm	23.50 38.30	48.50	74.00	173.40
5 µg/mg protein Emission at 515 nm Emission at 580 nm	39.80 15.80	17.30	23.30	50.30
1 µg/mg protein Emission at 515 nm Emission at 580 nm	53.30 9.10	7.80	6.13	13.10

Table 7.51. R.F.I. readings of
Free TRITC/Free FITC.

TRITC conc. plus 5 µg FITC/ mg protein.	R.F.I. at Excitation Wavelength		
	491 nm	499 nm	547 nm
25 µg/mg protein Emission at 515 nm	26.00		
Emission at 580 nm	81.00	81.00	443.00
5 µg/mg protein Emission at 515 nm	37.60		
Emission at 580 nm	24.00	24.00	112.00
1 µg/mg protein Emission at 515 nm	50.00		
Emission at 580 nm	13.00	13.00	36.00

Table 7.52. R.F.I. readings of
Free TRITC/Free FITC plus SDS.

7.5.3. Summary of Results.

From the results, it may be seen that fluorescence emission of the fluorescein chromophore, increases with decreasing original levels of TRITC for all three preparations. This clearly indicates that the fluorescein emission is being quenched by the TMR chromophore.

For the 25 µg/ml TMR/Fluorescein preparation in the absence of protein, it may be seen that addition of SDS produces more than 2½ times the intensity of emission when excited at 547 nm, compared with that in the absence of SDS. Similar results were obtained for conjugates containing lower levels of rhodamine. In the presence of SDS, the fluorescein chromophore does not elicit the usual decrease in fluorescence emission. The same finding was observed for all concentrations of TRITC.

Addition of SDS to the TMR/Fluorescein/anti-G1gG conjugate at a TMR concentration of 25 µg/ml, produces the

usual increase in emission intensity at 580 nm (when excited at 547 nm), of more than five-times that produced in the absence of SDS. Less dramatic results were observed at lower levels of TMR. For the fluorescein chromophore, addition of SDS decreases the intensity of fluorescence emission by approximately 54%. Similar results were observed at lower original levels of TRITC. The TMR/Fluorescein/anti-R1gG conjugate exhibited similar trends.

A possible explanation for the different behaviour exhibited in the emission of fluorescein when free, and when protein-bound in the presence of SDS, is that free FITC incubated with free TRITC is likely to produce covalent dimers, composed of one fluorescein and one TMR molecule.



Fig. 7.19. Reaction for the preparation of TMR/Fluorescein dimers.

Excitation at 491 nm will produce the excited state of fluorescein, and this excitation energy will be quenched by the attendant TMR molecule. Thus, fluorescein will exhibit vastly reduced levels of fluorescence emission.

Conversely, in the presence of protein, it is likely that FITC will bind to a lysine residue. This process will occur more readily than the covalent dimerisation process, since the ϵ -amino group of lysine is present at the start of the conjugation reaction; whereas hydrolysis of the isothiocyanate group to a primary amine takes time to occur. Thus,

protein-bound fluorescein may still be quenched by a TMR molecule but the latter will necessarily be more distant; perhaps on another lysine residue of the protein. As a consequence, quenching by energy transfer will be less efficient and therefore fluorescein will still show emission, and this may be quenched by the fluorescein aggregates whose production is promoted by SDS.

7.5.4. Conclusion.

It has been proposed that SDS dissociates TMR dimers into monomers, but promotes aggregation of fluorescein. From the data derived from the emission spectrum of TMR and fluorescein, it was seen that interaction of the former with SDS yields an increased relative fluorescence intensity, whereas interaction of SDS with the latter yields a decrease in the relative fluorescence intensity. It follows, therefore, that the dimers of TMR are themselves weakly fluorescent, and moreover, both species of dimer actively quench fluorescence emission of the monomer.

The quenching is thought to arise (39,40) as a result of direct inactive absorption by non-luminescent aggregates, and also transfer of excitation energy of monomers to them. It has been suggested (41) that in aggregates the $\phi_p : \phi_f$ ratio should also increase, where ϕ_p and ϕ_f are phosphorescence and fluorescence quantum yields, respectively.

For fluorescein, it is known (42) that excitation of its dimer results in dissociation to two monomers, since the first excited singlet state of the dimer is unstable. Dissociation

of the dimer releases non-radiative energy on its return to the ground state.

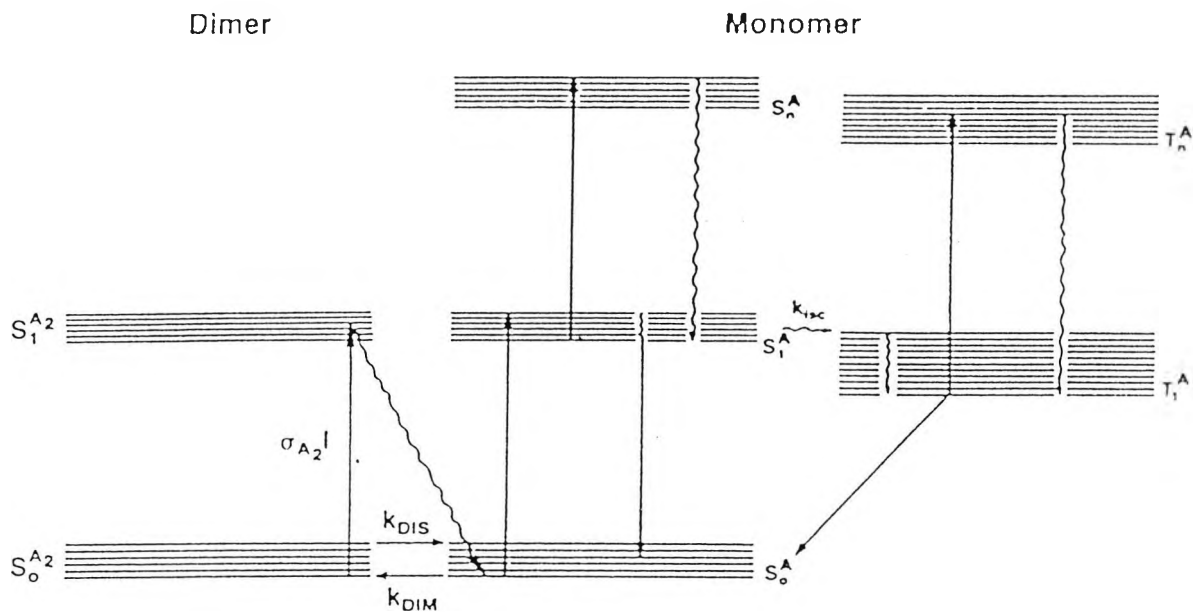


Fig. 7.20. Schematic Level Diagram for a dimer (A₂)-
(A₂)-monomer (A)/dye system. (→) and (↪) denote radiative and non-radiative transition
respectively. k_{isc} denotes the intersystem crossing rate. Dissociation of the dimer at
its S₁ state is fast compared to the excitation process (42).

7.6. REFERENCES.

1. Kautsky, H.
(1939) Trans. Farad. Soc. 35 216
2. Knibbe, H., Rehm, D. & Weller, A.
(1968) Ber. Bunsenges 72 257
3. Lehrer, S.S.
(1971) Biochemistry 10 3254
4. Horrocks, A.R., Kearvell, A., Tickle, K. & Wilkinson, F.
(1966) Trans. Farad. Soc. 62 3393
5. Cavatorta, P., Favilla, R. & Mazzini, A.
(1979) Biochim. Biophys. Acta 578 541
6. Winkler, M.H.
(1969) Biochemistry 8 2586
7. Dreeskamp, H., Koch, E. & Zander, M.
(1975) Naturforsch 30a 1311
8. Green, J.A., Singer, L.A. & Parks, J.H.
(1973) J. Chem. Phys. 58 2690
9. Ware, W.R., Watt, D. & Holmes, J.D.
(1974) J. Amer. Chem. Soc. 96 7853
10. Taylor, G.N.
(1971) Chem. Phys. Lett. 10 355
11. Kasha, M.
(1952) J. Chem. Phys. 20 71
12. Medinger, T. & Wilkinson, F.
(1965) Trans. Farad. Soc. 61 620
13. Eftink, M.R., Zajicek, J.L. & Ghiron, C.A.
(1977) Biochim. Biophys. Acta 491 473
14. Lakowicz, J.R. & Anderson, C.J.
(1980) Chem. Biol. Interactions 30 309
15. Forster, Th.
(1948) Annalen der Physik (Leipzig) 2 55
English Translation: Sinclair, D.A.
(1955) National Research Council of Canada
Technical Translation TT 564 pp 1-36

16. Wu, C.-W. & Stryer, L.
(1972) Proc. Natl. Acad. Sci. USA 69 1104
17. Katchalski-Katzir, E., Haas, E. & Steinberg, I.Z.
(1981) Ann. N.Y. Acad. Sci. 366 44
18. Haas, E., Wilchek, M., Katchalski-Katzir, E.
& Steinberg, I.Z.
(1975) Proc. Natl. Acad. Sci. USA 72 1807
19. Grinvald, A., Haas, E. & Steinberg, I.Z.
(1972) Proc. Natl. Acad. Sci. USA 69 2273
20. Haas, E., Katchalski-Katzir, E. & Steinberg, I.Z.
(1978) Biopolymers 17 11
21. Rabinowitch, E. & Epstein, L.F.
(1941) J. Amer. Chem. Soc. 63 69
22. Ferguson, J. & Mau, A.W.H.
(1972) Chem. Phys. Lett. 17 543
23. Brandtzaeg, P.
(1975) Ann. N.Y. Acad. Sci. 254 35
24. McKinney, R.M. & Spillane, J.T.
(1975) Ann. N.Y. Acad. Sci. 254 55
25. Goding, J.W.
(1976) J. Immunol. Methods 13 215
26. Arbeloa, I.L.
(1981) J. Chem. Soc. Farad. Trans. 2 77 1725
27. Cebra, J.J. & Goldstein, G.
(1965) J. Immunol. 95 230
28. Amante, L., Ancona, A. & Forni, L.
(1972) J. Immunol. Methods 1 289
29. Canfield, R.E.
(1963) J. Biol. Chem. 238 2698
30. Chen, R.F.
(1970) Biochem. Biophys. Res. Commun. 40 1117
31. Aboderin, A.A. & Boedefeld, E.
(1976) Biochim. Biophys. Acta 420 177

32. Kelkar, V.K., Valaulikar, B.S., Kunjappu, J.T. & Manohar, C.
(1990) Photochem. Photobiol. 52 717
33. Pant, D.D. & Pant, H.C.
(1968) Indian J. Pure Appl. Physics 6 238
34. Rohatgi, K.K. & Mukhopadhyay, A.K.
(1972) J. Phys. Chem. 76 3970
35. Mukerjee, P. & Ghosh, A.K.
(1970) J. Amer. Chem. Soc. 92 6403
36. Kasha, M.
(1963) Radiat. Res. 20 55
37. Valdes-Aguilera, O. & Neckers, D.C.
(1989) Acc. Chem. Res. 22 171
38. Arbeloa, I.L. & Ojeda, R.P.
(1982) Chem. Phys. Lett. 87 556
39. Levshin, V.L. & Boranova, E.G.
(1959) Optics & Spectroscopy N.Y. 6 31
40. Boranova, E.G. & Levshin, V.L.
(1961) Optics & Spectroscopy 10 182
41. McRae, E.G. & Kasha, M.
(1958) J. Chem. Phys. 28 721
42. Speiser, S., Houlding, V.H. & Yardley, J.T.
(1988) Appl. Physics B 45 237

CHAPTER 8.

INVESTIGATION INTO THE NATURE OF THE FLUORESCENCE QUENCHING
OF AN EXTRINSIC FLUOROPHORE BY THE HAEM MOIETY IN
HORSERADISH PEROXIDASE.

8.1. DISCOVERY OF HORSERADISH PEROXIDASE.

In 1863 it was observed (1), that animal and vegetable extracts possessed peroxidative properties. These properties were later attributed (2) to special, indirect oxidising enzymes, and the latter were subsequently given the general name of 'peroxidases' (3). Some twenty-five years later, an enzyme in this category was isolated and purified to 40% homogeneity (4).

It was later found (5), that two forms of peroxidase may be isolated from horseradish roots. These were designated true peroxidase and 'paraperoxidase.' Using carboxymethyl cellulose chromatography, five forms (isoenzymes) of peroxidase were isolated (6) from horseradish. These were called A, B, C, D and E. Diethylaminoethyl (DEAE) cellulose chromatography of peroxidase A (7), yielded three fractions designated A1, A2 and A3.

8.2. LOCATION, ISOLATION & PURIFICATION OF HORSERADISH PEROXIDASE.

Horseradish (*Armoracia rusticana*) roots (7), were cut into cubes and homogenised in the presence of potassium phosphate buffer. The homogenate was filtered, treated with ammonium sulphate, centrifuged, and the supernatant was isolated and treated with excess ammonium sulphate. After standing overnight, the residue was collected by centrifugation and redissolved in Tris buffer.

The crude preparation (8), was subjected to chromatography

on carboxymethyl- or DEAE-cellulose, and the issuing isoenzyme fractions were pooled. The resulting mixtures were dialysed against water and lyophilised. The lyophilised enzyme preparations were dissolved in sodium acetate buffer to a final protein concentration of approximately 50 mg/ml. An aliquot of this solution, was subjected to gel filtration. Fractions were collected and subjected to Ultra Violet spectral analysis.

The ratio of absorption of the Soret band (peak at 403 nm) to that at 275 nm, for each fraction were measured. The ratio is referred to as the 'Reinheitszahl' or RZ value (9). Fractions with high RZ values; 4.0 for isoenzymes A1 and A2, 3.5 for isoenzyme A3, and 3.3 for isoenzymes B and C, were pooled, lyophilised and further purified by preparative column electrophoresis (10).

8.3. CHEMICAL & PHYSICAL PROPERTIES OF HORSERADISH PEROXIDASE.

It was found (11), that extracts of horseradish root possessed porphyrin, and this latter component was found in enzyme preparations of different purities (12,13,14). This observation led to the suggestion that the porphyrin is a component of horseradish peroxidase, and this proposal was later confirmed (15), by the investigation of the interaction of horseradish peroxidase with its substrates.

Horseradish peroxidase (HRP) shares certain features with other proteins, such as catalase and methaemoglobin. All are haemoproteins containing an identical prosthetic

group; iron protoporphyrin IX or haem, united to different proteins.

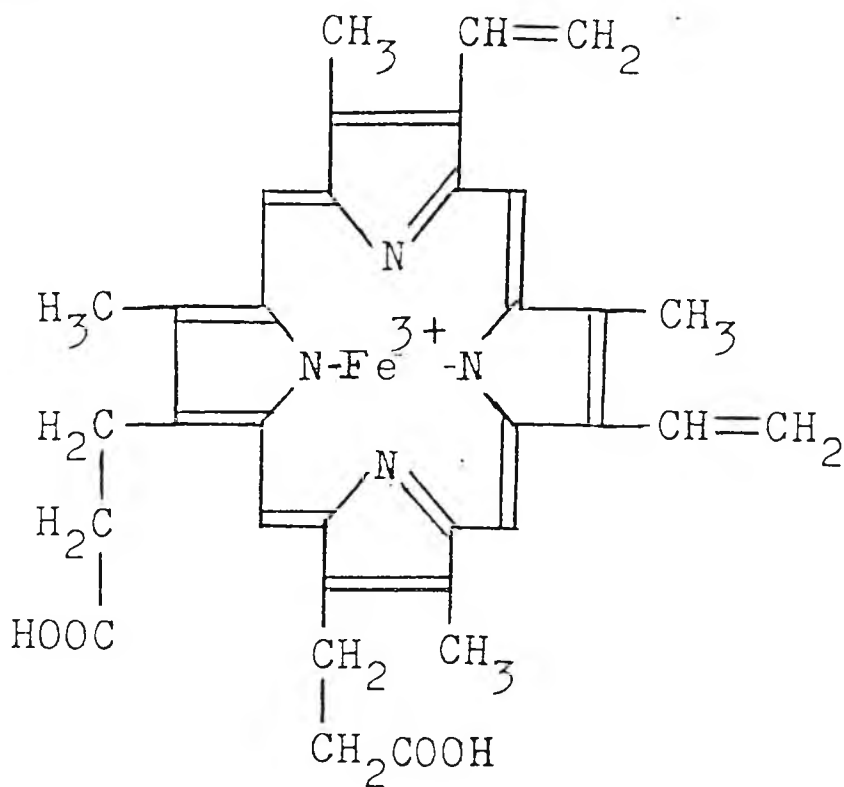


Fig. 8.1. Iron Protoporphyrin IX or Haem.

The iron atom is in the tri-valent state, and their colour and the general description of their absorption spectra are akin to those of acid methaemoglobin.

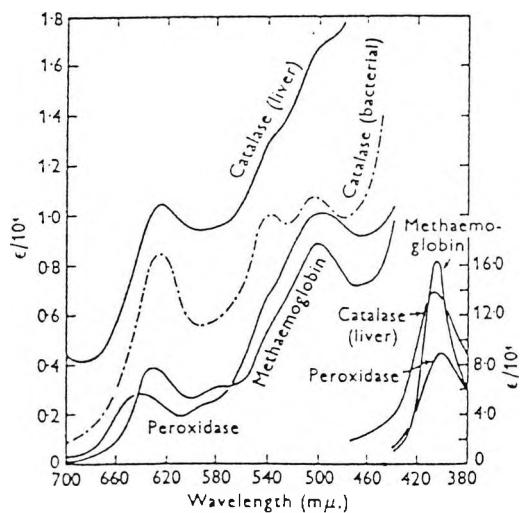


Fig. 8.2. Absolute absorption spectra of methaemoglobin, peroxidase and liver catalase (16), together with the corresponding curve for bacterial catalase (17).

All three haemoproteins react reversibly with a variety of simple inorganic compounds, forming spectroscopically well-defined compounds. The stoichiometry of binding is one molecule of reactant per iron atom.

The most striking difference in the properties of these three haemoproteins, is found in the magnitude of their catalytic activities. Whereas peroxidase and catalase are very powerful catalysts, methaemoglobin shows only slight peroxidatic and catalytic activities.

Horseradish peroxidase (Donor : hydrogen peroxidase oxidoreductase, E.C. No. 1.11.1.7), is a plant glycoprotein, composed of more than twenty isoenzymes (18) with isoelectric points (pI) ranging from 3.5 to 9.0. The isoenzymes containing most of the peroxidase activity have isoelectric points between 5.5 and 7.6. The enzyme possesses a sedimentation constant of 3.48×10^{-13} second, (3.48 S), (19).

Horseradish peroxidase isoenzyme C (HRP-C) dominates quantitatively among the isoperoxidases of horseradish root, and has an isoelectric point close to 9.0. It is composed of 308 amino acid residues including four disulphide bridges in a single polypeptide chain, that carries eight neutral carbohydrate side chains.

It has been shown (20) that calcium contributes to the structural stability, and hence enzymatic activity, of the protein. Isoenzymes C and A contain 2.0 and 1.4 moles of calcium per mole enzyme, respectively. The calcium may be removed by incubation with aqueous guanidinium hydrochloride (6 M) and EDTA. Calcium-free isoenzyme C reconstitutes upon

addition of calcium, and regains enzymatic activity, whereas calcium-free isoenzyme A will not readily reconstitute in the presence of calcium.

8.4. PRIMARY STRUCTURE OF HRP.

HRP-C possesses a molecular weight of 33890 daltons, as calculated from its amino acid sequence. Assuming an average carbohydrate composition of (N-acetyl-glucosamine)₂, (mannose)₃, fucose and xylose for each carbohydrate chain, the molecular weight of native HRP-C is close to 44000 daltons (21).

	5	10	carb	15	20	25		
[Glu-Leu-Thr-Pro-Thr-Phe-Tyr-Asp-Asn-Ser-Cys-Pro-Asn-Val-Ser-Asn-Ile-Val-Arg-Asp-Thr-Ile-Val-Asn-Glu-							
	30	35		40	45	50		
	Leu-Arg-Ser-Asp-Pro-Arg-Ile-Ala-Ala-Ser-Ile-Leu-Arg-Leu-His-Phe-His-Asp-Cys-Phe-Val-Asn-Gly-Cys-Asp-							
	55	carb	60	65	70	75		
	Ala-Ser-Ile-Leu-Leu-Asp-Asn-Thr-Thr-Ser-Phe-Arg-Thr-Glu-Lys-Asp-Ala-Phe-Gly-Asn-Ala-Asn-Ser-Ala-Arg-							
	80		85	90	95	100		
	Gly-Phe-Pro-Val-Ile-Asp-Arg-Met-Lys-Ala-Ala-Val-Glu-Ser-Ala-Cys-Pro-Arg-Thr-Val-Ser-Cys-Ala-Asp-Leu-							
	105		110	115	120	125		
	Leu-Thr-Ile-Ala-Ala-Gln-Gln-Ser-Val-Thr-Leu-Ala-Gly-Gly-Pro-Ser-Trp-Arg-Val-Pro-Leu-Gly-Arg-Arg-Asp-							
	130		135	140	145	150		
	Ser-Leu-Gln-Ala-Phe-Leu-Asp-Leu-Ala-Asn-Ala-Asn-Leu-Pro-Ala-Pro-Phe-Phe-Thr-Leu-Pro-Gln-Leu-Lys-Asp-							
	155	carb	160	165	170	175		
	Ser-Phe-Arg-Asn-Val-Gly-Leu-Asn-Arg-Ser-Ser-Asp-Leu-Val-Ala-Leu-Ser-Gly-Gly-His-Thr-Phe-Gly-Lys-Asn-							
	180		185 carb	190	195	carb	200	
	Gln-Cys-Arg-Phe-Ile-Met-Asp-Arg-Lou-Tyr-Asn-Phe-Ser-Asn-Thr-Gly-Leu-Pro-Asp-Pro-Thr-Leu-Asn-Thr-Thr-							
	205		210	carb	215	220	225	
	Tyr-Leu-Gln-Thr-Leu-Arg-Gly-Leu-Cys-Pro-Leu-Asn-Gly-Asn-Leu-Ser-Ala-Leu-Val-Asp-Phe-Asp-Leu-Arg-Thr-							
	230		235		240	245	250	
	Pro-Thr-Ile-Phe-Asp-Asn-Lys-Tyr-Tyr-Val-Asn-Leu-Glu-Glu-Gln-Lys-Gly-Leu-Ile-Gln-Ser-Asp-Gln-Glu-Leu-							
	carb		260		265	carb	270	275
	Phe-Ser-Ser-Pro-Asn-Ala-Thr-Asp-Thr-Ile-Pro-Leu-Val-Arg-Ser-Phe-Ala-Asn-Ser-Thr-Gln-Thr-Phe-Phe-Asn-							
	280		285		290	295	300	
	Ala-Phe-Val-Glu-Ala-Met-Asp-Arg-Met-Gly-Asn-Ile-Thr-Pro-Leu-Thr-Gly-Thr-Gln-Gly-Gln-Ile-Arg-Leu-Asn-							
	305							
	Cys-Arg-Val-Val-Asn-Ser-Asn-Ser							

Disulfide bridges: 11-91, 44-49, 97-301, 177-209.

Fig. 8.3. The amino acid sequence of horseradish peroxidase, carb = site of carbohydrate attachment (22).

The eight sites of carbohydrate attachment are all present as Asparagine-(carbohydrate)-X-Serine/Threonine, X being any residue. The amino-terminus was found to be blocked in the form of a pyrrolidonecarboxyl residue, and the carboxyl-terminal serine residue is easily lost, indicating lability of the asparaginyl-serine peptide bond (23).

8.5. HOMOLGY BETWEEN HRP-C AND OTHER HAEMOPROTEINS.

Since, as already discussed, it is known that HRP possesses spectral and catalytic properties in common with animal proteins, for example, haemoglobin, similarities in the primary structures of various haemoproteins were investigated. It was found (24) that an invariable histidine residue is present as the fifth ligand of haem iron (proximal histidine), and an almost invariable histidine (distal histidine) occupied a position close to the sixth co-ordination position. The primary structure of a number of plant peroxidases show two conserved histidine sequences (25). One histidine sequence of these enzymes has four conserved residues in common with the proximal globin sequences: Leu-Xaa-Xaa-Leu-Ser-Xaa-Xaa-His (invariable residues underlined) and these correspond to residues 163 to 170 of HRP-C. The other histidine sequence shares a similar hydrophobic pattern and two residues with the distal globin sequences: Leu-Xaa-Xaa-His, and these correspond to residues 39 to 42 of HRP-C.

Thus, for HRP-C, the distal histidine residue is present at position 42. It is also in this position for turnip

peroxidase (TP-7), but is present at position 52 in yeast cytochrome c peroxidase (CCP). For HRP-C, the proximal histidine residue is present at position 170, whilst for TP-7 and CCP, the positions are 159 and 175, respectively.

It has been shown (26), that the primary structure of CCP and HRP-C possess 15% identity. The primary structures of HRP-C, TP-7 and CCP are aligned as shown, using the distal and proximal histidine residues as starting points.



Fig. 8.4. Alignment of horseradish peroxidase HRP-C, turnip peroxidase TP-7 and yeast cytochrome c peroxidase CCP amino acid sequences, and predicted or observed secondary structure (27). Amino acid sequences are in the IUB-IUPAC single letter notation (28). Glycosylated residues of HRP-C are encircled. The first line in each train of alignment, notifies sequence identities of plant and yeast peroxidases; capitals indicate identity of all three, and small letters indicate identity of yeast and only one plant peroxidase. In the second line (-) notifies identical residues in the two plant peroxidases. Line five shows predicted secondary structure in plant peroxidases; (o) for helix, (-) for extended, and (') for reverse turn. The last line notifies secondary structure (predominantly helices A to J1), observed in the crystal structure of CCP.

In this alignment, CCP is 18% identical to HRP-C, 16% identical to TP-7 and 12% of the residues, (40 out of 324 positions) are identical in all three proteins.

8.6. THE SECONDARY STRUCTURE OF HRP.

Circular dichroism spectra of peroxidase isoenzymes of horseradish (29), turnip (30) and Japanese radish (31), are so similar that the secondary structures must be almost identical. In view of this, a general structural model for plant peroxidases has been represented.

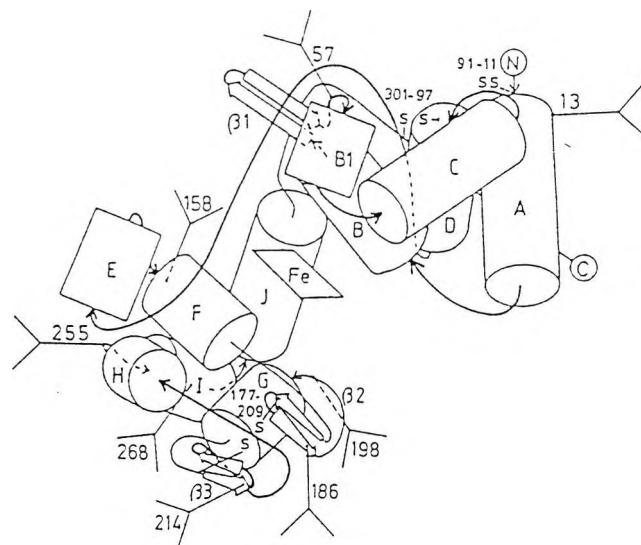


Fig. 8.5. Structural model of peroxidase (27). Helices A to J are drawn as cylindrical projections. Extended structures $\beta 1$, $\beta 2$ and $\beta 3$ are shown as arrows. Reverse turns and coil are shown as connecting lines. The two domains of the peroxidase, enclosing the central haem prosthetic group (Fe in a rectangle), are spaced out for clarity. The amino- and carboxyl-terminals are indicated by N and C respectively. Three disulphide bridges of plant peroxidases are indicated by -SS-, and by the residue numbers of the corresponding half-cystines of HRP-C. The eight carbohydrate moieties are indicated by numbers and a symbolic fork.

From Fig. 8.4., it may be seen that three of the four disulphide bridges in HRP-C and TP-7, are formed from sequentially distant residues: 11-91, 97-301 and 177-209 in HRP-C. Residues 11 and 91 correspond to the beginning of helix A and the end of helix C, respectively. Residues 97 and 301 correspond to the beginning of helix D and eight residues before the carboxyl-terminus of HRP-C, respectively. Both of these pairs are close in space, allowing disulphide linkage to occur. Residues 177 and 209 correspond to the turn in β_2 and the beginning of β_3 . The general structural model (Fig. 8.5), shows that these residues are not close enough for disulphide bridge formation. However, Fig. 8.4. demonstrates that the area of the homologous primary sequence exhibits great differences in the primary structure, between the three proteins. It is probable, therefore, that the general structural model does not allow for disulphide bridge formation, but that deviations from the general model will allow formation of the disulphide linkage, between the residues concerned.

The crystal structure of yeast cytochrome c peroxidase (32), suggested a definite division of the molecule into two domains, separated by the haem moiety. Domain I comprised helices A, B, C and D (which corresponds to residues 1-144 of HRP-C), and a carboxyl-terminal 'arm', whilst domain II consisted of helices F to J, (which corresponds to HRP-C residues 158-289).

Mild tryptic digestion of horseradish apo-peroxidase, (that is, enzyme devoid of the haem moiety) leading to partial

cleavage, gave rise to a two-domain structure. The 'distal' domain comprising residues 1-149 and 265-308, was quite resistant to degradation and the core of the 'proximal' domain comprising residues 160-224, was very resistant to proteolysis.

These observations indicate that both yeast and plant peroxidases share common primary, secondary and ultimately, tertiary structural features.

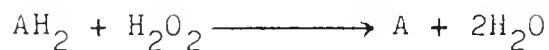
8.7. FUNCTION & MECHANISM OF ACTION OF HRP.

The haem moiety has been implicated in the mechanism of HRP action by the following observations:

- i) all preparations; from horseradish root itself to the most highly purified enzyme, were found to contain a porphyrin whose absorption spectrum resembled that of acid methaemoglobin;
- ii) proportionality was observed between the intensity of the absorption spectrum of the porphyrin, and the potency of the enzyme preparation;
- iii) spectroscopically well-defined compounds were observed between the porphyrin and inhibitors of the enzyme;
- iv) formation of well-defined compounds between the porphyrin and the reactant for the enzyme was noted;
- v) rapid decomposition of the porphyrin-reactant complex was seen, on addition of substrates, for example, pyrogallol, quinol, ascorbic acid, etc.

Horseradish peroxidase, and other classical haemoprotein peroxidases which have a histidine residue as the fifth haem ligand, catalyse the oxidation of organic substrates with

hydrogen peroxide as the reactant. The H_2O_2 acts as the ultimate electron acceptor (33).



In contrast, cytochrome P-450 enzymes, which have a cysteine thiolate as the fifth ligand, generally transfer oxygen from molecular oxygen or alternative oxygen donors to their substrates (34). The active oxidant in both the peroxidases and P-450 monooxygenases, is thought to be a ferryl complex known as Compound I, which is two oxidation equivalents above the ferric resting state. Compound I is then reduced back to the Fe^{3+} state in two steps through Compound II.

Horseradish peroxidase catalyses some oxygen-incorporating reactions, including the epoxidation of styrene, which require a co-substrate (co-oxidations), and involve the one-electron oxidation of the co-substrate to a radical that reacts with O_2 to form a peroxy-radical (ROO^\bullet), which is responsible for product formation (35).

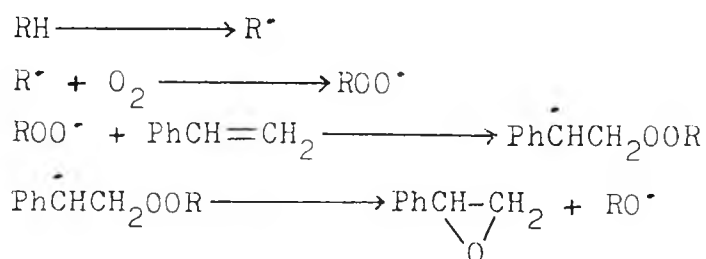


Fig. 8.6. Mechanism for the epoxidation of styrene.

The co-substrate (RH), is oxidised to a radical (R^\bullet) which reacts with molecular oxygen. The resulting peroxy-radical

(ROO^\bullet) then adds to the double bond of styrene, to produce an organo-peroxy carbon radical ($\text{PhCHCH}_2\text{OOR}$) that decomposes to styrene oxide and the alkoxy radical (RO^\bullet).

Horseradish peroxidase also catalyses a variety of reactions including the N-dealkylation of alkylamines, (36) the hydroxylation of a benzylic methyl group (37) and the conversion of sulphides to sulphoxides (38,39). In all cases, except the latter, the source of the incorporated oxygen atom is not H_2O_2 ; thus, these reactions are thought not to proceed via oxo-transfer from Compound I. This indicates that additional factors other than just the metal co-ordination structure must play a role in controlling the modes of reactions of the enzyme intermediates.

It has been suggested (40), that horseradish peroxidase, and possibly other classical peroxidases, differ from the monooxygenases in that substrates are prevented from reacting with the ferryl oxygen, and are only allowed to react with the edge of the prosthetic haem group. This is achieved, in HRP, by the imposition of a physical barrier between the substrate and the ferryl oxygen.

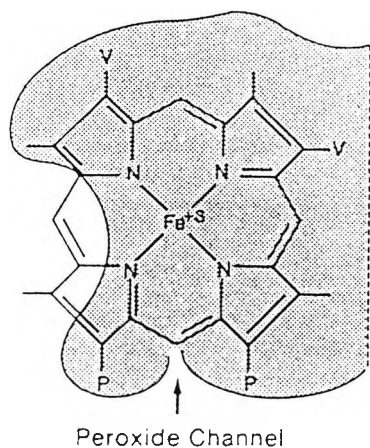


Fig. 8.7. Model of the active site proposed for horseradish peroxidase, showing the exposed sector of the prosthetic haem to which electrons are transferred from the substrate (40).

The existence of a solvent exposed haem edge is supported by the finding that Compound I and ferric HRP, disproportionates to two molecules of Compound II (46).

8.8. FLUORESCENT MODIFICATION OF HRP-C USING FLUORESCHEIN ISOTHIOCYANATE.

The haem moiety of HRP may accept excited state energy from both intrinsic fluorescent amino acid residues (for example, Phe, Tyr, Trp) as well as a covalently attached extrinsic fluorophore. Experimental procedures were undertaken in order to investigate the nature of the latter phenomenon.

From the primary structure, it may be seen that HRP-C possesses six lysine residues. It has been shown (47) that the extent of lysine modification may be varied by altering the conditions of temperature and pH of the conjugation medium. At 40°C and at pH 8.5, all six lysine residues may be modified with trinitro-benzenesulphonic acid (TNBS), within two hours.

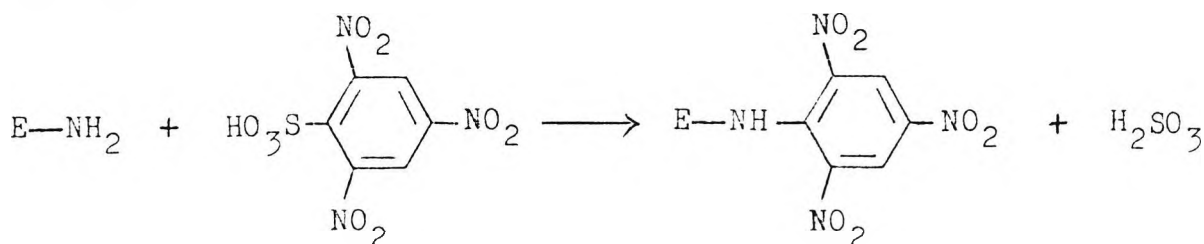


Fig. 8.10. Modification of the ϵ -amino group of lysine by TNBS.

At 22°C and at pH 9.5, four of the lysine residues may be transformed with TNBS, within one hour, whilst at 0°C at pH 8.5, three of the lysine residues may be modified with TNBS within

two hours. In view of this finding, partial modification of HRP-C with fluorescein isothiocyanate (FITC) was attempted.

8.8.1. Experimental Procedure.

Refined HRP-C (RZ value, 3.2) (1.0 mg) was dissolved in Tris-HCl/KCl buffer (0.20 M, 0.50 ml, pH 8.0).

FITC (0.50 mg; 1.29 μmol) was dissolved in acetonitrile (50 μl). These solutions were then incubated in ice until they reached a temperature of 0°C ; they were then thoroughly mixed, and ice-cold Tris-HCl/KCl buffer (0.45 ml) was then added.

The resultant solution was allowed to stand for 10 minutes at 0°C , and a large excess of n-butylamine was then added in order to terminate the conjugation process. The conjugation medium was then applied to a Sephadex G-25 gel exclusion chromatographic column (20-80 μm bead size, bed volume: approximately 10 ml), which had previously equilibrated with phosphate buffer (0.10 M, pH 7.4), and was eluted with this buffer.

The protein-containing fraction was collected and diluted to 2 ml with the phosphate buffer. This solution was then divided into two equal portions. The haem moiety from one portion, was then removed utilising a documented procedure (48). To this portion was added dilute hydrochloric acid (0.10 M) drop-wise until the sample reached pH 2.0, (approximately 15 drops). An equal total volume of ice-cold methyl ethyl ketone was added, and the mixture was shaken. On partition, it was seen that the upper ketonic layer assumed a reddish colouration

which was due to the haem moiety. This layer was decanted, and a second portion of ice-cold methyl ethyl ketone was added, and this was decanted likewise. The decanted portions were pooled, and a visible spectrum was scanned. A peak absorbance at 403 nm confirmed the presence of haem.

The two portions (that is, ketone treated HRP (apo-enzyme) and intact HRP (holo-enzyme)) were then dialysed extensively (3 days) against phosphate buffer (0.10 M, 1000 ml, pH 7.4), using cellulose tubing which retains molecular weight species in excess of 12000 daltons. The solutions were then diluted to 3 ml with the phosphate buffer, and were then subjected to U.V./visible and fluorescence spectral analysis.

8.8.2. Results.

It may be seen that the FITC conjugates absorbed maximally at 491 nm. The holo-enzyme portion exhibited a peak at 403 nm, due to the haem moiety. No such peak was evident in the apo-enzyme preparation.

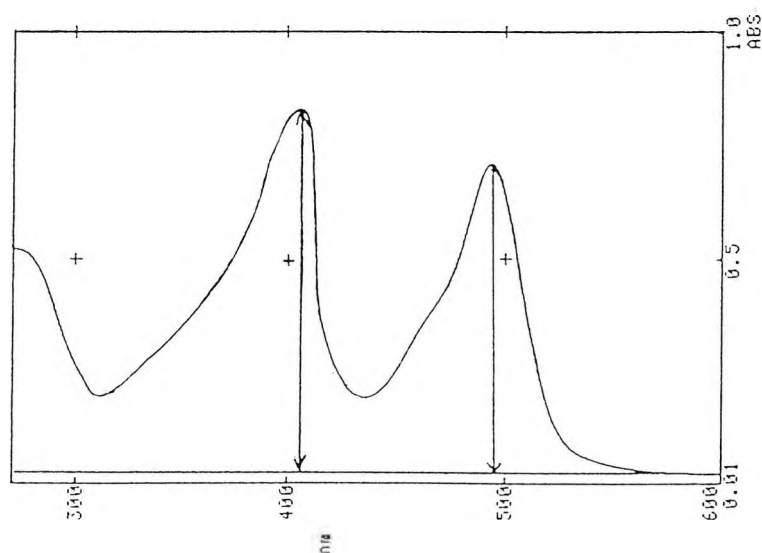


Fig. 8.11. U.V./visible spectrum of FITC/HRP-C conjugate. Since the haem moiety absorbs far into the red, the FITC peak was baselined against haem solution of equal absorbance at 403 nm.

8.8.3. Calculation of the Stoichiometry of the FITC/HRP-C Conjugate.

From the Beer-Lambert law, $D = \epsilon \cdot c \cdot l$

For a pathlength of 1 cm, $D = \epsilon \cdot c$

$$c = \frac{D}{\epsilon}$$

For the probe, $c = \frac{0.700}{\epsilon \text{ at } 491 \text{ nm}}$ $\epsilon \text{ at } 491 \text{ nm} = 72000$
(Ref. 49)

$$c = \frac{0.700}{72000} = 9.7 \times 10^{-6} \text{ M.}$$

For the protein, $c = \frac{0.760}{\epsilon \text{ at } 403 \text{ nm}}$ $\epsilon \text{ at } 403 \text{ nm} = 91000$
(Ref. 50)

$$c = \frac{0.760}{91000} = 8.4 \times 10^{-6} \text{ M.}$$

Thus, the dye : protein ratio is 1 : 1.

8.8.4. Summary of Results.

All solutions were adjusted to give an absorbance of 0.10 at 491 nm, and the adjusted solutions were then excited at this wavelength for fluorescence spectral analysis.

Both samples exhibited an emission maximum at 515 nm, due to the fluorescein moiety. The relative fluorescence intensity of the intact HRP preparation was found to be approximately 171, whilst that of the apo-enzyme was calculated to be 2050.

Thus, it is evident that the haem moiety exerts a

fluorescence quenching effect over the fluorescein label, since a fluorescence increase of approximately 1200% was observed for the preparation devoid of haem. The absorption of the acceptor (haem) exhibits a peak at 403 nm, and the emission of the donor (fluorescein) exhibits a peak at 515 nm, and consequently there is quite a large gap (112 nm) between the peaks. However, the absorption spectrum of the haem is very broad, and is still absorbing far into the red portion of the spectrum. As a result, haem is a potent quencher of fluorescence emission via energy transfer.

8.9. CORRELATION BETWEEN THE RZ VALUE OF THE PROTEIN AND THE EXTENT OF FLUORESCENCE QUENCHING OF Ru COMPLEX I.

8.9.1. Experimental Procedure.

Various grades of HRP-C were obtained, possessing RZ values of 0.5, 1.1 and 3.2. These samples were designated Type I, II and III, respectively. Bis (1,10-phenanthroline) (Bathophenanthroline disulphonyl chloride) ruthenium (II) hexafluorophosphate dihydrate (Ru Complex I), was utilised as synthesised. The partial modification of these enzymes utilising Ru Complex I (1.0 mg; 1.0 μ mol/mg protein), and subsequent removal of the haem moiety was performed as previously described in Section 8.8.1.

8.9.2. Results.

Type I Holo-enzyme Bound Probe:	Peak Emission = 625 nm
	Peak Absorbance = 433 nm
	Stokes Shift = 192 nm
	Relative Fluorescence Intensity = 261

Type I Apo-enzyme Bound Probe:

Relative Fluorescence Intensity = 271

Fluorescence Change = +3.83%

Type II Holo-enzyme Bound Probe: Peak Emission = 625 nm

Peak Absorbance = 433 nm

Stokes Shift = 192 nm

Relative Fluorescence Intensity = 260

Type II Apo-enzyme Bound Probe:

Relative Fluorescence Intensity = 282

Fluorescence Change = +8.46%

Type III Holo-enzyme Bound Probe: Peak Emission = 625 nm

Peak Absorbance = 433 nm

Stokes Shift = 192 nm

Relative Fluorescence Intensity = 266

Type III Apo-enzyme Bound Probe:

Relative Fluorescence Intensity = 323

Fluorescence Change = +21.43%

All probe : protein ratios were found to be 1 : 1.

8.9.3. Conclusion.

It is seen that there is a correlation between the RZ value of the protein and the extent of fluorescence quenching of the Ru Complex I. This demonstrates that the haem moiety is responsible for the fluorescence quenching of the extrinsic fluorophore. Also, it is evident that the more inferior grades of commercially available HRP, either possess defective haem centres or the haem moiety is absent altogether.

It may be seen that the haem moiety of HRP-C, accepts excited state energy more effectively from the fluorescein chromophore than from the ruthenium complex chromophore. This

may be a consequence of the greater overlap integral, J , between the absorption spectrum of the haem moiety, and emission spectrum of the fluorescein ($J = 8.17 \times 10^{-15} \text{ cm}^3/\text{mol}$) as compared to that of Ru Complex I ($J = 1.80 \times 10^{-16} \text{ cm}^3/\text{mol}$).

8.10. DETERMINATION OF THE DISTANCE BETWEEN THE HAEM MOIETY AND THE COVALENT FLUOROPHORE.

The determination of the relative fluorescence intensity of an extrinsic fluorescent probe, both in the presence and absence of the haem moiety, will allow the calculation of the distance between the haem moiety and the attendant fluorophore.

The efficiency of energy transfer (E) may be calculated from the relative fluorescence intensity of the donor, both in the presence (F_{da}) and absence (F_d) of acceptor, by the following relationship:

$$E = 1 - (F_{da}/F_d)$$

The efficiency of energy transfer may then be related to the distance between the donor and acceptor via:

$$E = \frac{R_0^6}{R_0^6 + r^6}$$

where R_0 is the distance at which 50% quenching efficiency is achieved, and r is the distance between the donor and acceptor molecules. R_0 may be calculated from the equation:

$$R_0^6 \text{ (cm)} = 8.8 \times 10^{-25} (K^2 \cdot J \cdot n^{-4} \cdot \phi_d)$$

where K^2 is a factor describing the relative orientation in space of the transition dipoles of the donor and acceptor, and is normally ascribed a value of 0.67 for a substantially randomised angular relationship between the donor and acceptor, during the excited state lifetime (51); J , the overlap integral which expresses the degree of spectral overlap between the donor emission and the acceptor absorption, has been determined as $8.17 \times 10^{-15} \text{ cm}^3/\text{mol}$, from the appropriate spectra of haem and fluorescein; n is the refractive index of the medium, and is ascribed a value of 1.4 (51); the quantum yield, ϕ_d , of the donor in the reaction medium was found to be 0.38 assuming a quantum yield of 0.85 for fluorescein in NaOH solution (0.10 M), for equivalent absorbance at 450 nm (52).

$$\begin{aligned} \text{Thus, } R_o^6 \text{ (cm)} &= 8.8 \times 10^{-25} (K^2 \cdot J \cdot n^{-4} \cdot \phi_d) \\ &= 8.8 \times 10^{-25} (0.67 \times 8.17 \times 10^{-15} \times 0.26 \times 0.38) \\ &= 4.76 \times 10^{-40} \end{aligned}$$

$$\text{Thus, } R_o \text{ (cm)} = 2.79 \times 10^{-7} = \underline{27.9 \overset{\circ}{\text{A}}}$$

Therefore, the transfer efficiency is 50% when the distance between the donor and acceptor is approximately $28 \overset{\circ}{\text{A}}$.

$$\begin{aligned} E &= 1 - (F_{da}/F_d) \\ &= 1 - (171/2050) \\ 0.92 &= \frac{R_o^6}{R_o^6 + r^6} \end{aligned}$$

$$0.92 = \frac{(27.9)^6}{(27.9)^6 + r^6}$$

$$\text{Thus, } r^6 = 4.06 \times 10^7 \text{ \AA}^6$$

$$r = \underline{18.54 \text{ \AA}}$$

For the Ru Complex I-Type III HRP-C conjugate (RZ value 3.2), where J was found to be $1.80 \times 10^{-16} \text{ cm}^3/\text{mol}$ and ϕ_d for the probe under the same conditions as fluorescein (52), was found to be 0.23.

$$\begin{aligned} \text{Thus, } R_0^6 \text{ (cm)} &= 8.8 \times 10^{-25} (0.67 \times 1.80 \times 10^{-16} \times 0.26 \times 0.23) \\ &= 6.35 \times 10^{-42} \end{aligned}$$

$$R_0 \text{ (cm)} = 1.36 \times 10^{-7} = \underline{13.6 \text{ \AA}}$$

Therefore, the transfer efficiency is 50% when the distance between the donor and acceptor is approximately 14 \AA.

$$E = 1 - (266/323)$$

$$0.19 = \frac{(13.6)^6}{(13.6)^6 + r^6}$$

$$r^6 = 2.9 \times 10^7 \text{ \AA}^6$$

$$r = \underline{17.51 \text{ \AA}}$$

The distance, r, may be verified by the determination of the excited state lifetime of an extrinsic fluorophore (donor), both in the presence and absence of the energy acceptor; since the efficiency of energy transfer (E) may also be calculated from the excited state lifetimes of the donor

in the presence (T_{da}) and absence (T_d) of acceptor by the following relationship:

$$E = 1 - (T_{da}/T_d).$$

8.10.1. Experimental Procedure.

The partial modification of HRP-C (Type III, RZ value, 3.2) utilising Ru Complex I as synthesised, and subsequent removal of the haem moiety was performed as previously described in Section 8.8.1.

The dye : protein ratio was found to be 1 : 1. As a comparison, Ru Complex I (0.50 mg) was dissolved in acetonitrile (25 μ l), and to this solution was added n-butylamine (250 μ l), followed by phosphate buffer (0.10 M, 725 μ l, pH 7.4). This solution was utilised as free Ru Complex I. All solutions were deoxygenated via the passage of argon through the samples for at least 15 minutes. Fluorescent lifetime measurements were immediately recorded.

8.10.2. Results.

It was found that the Ru Complex I labelled holo-enzyme (intact HRP-C) exhibited an excited state lifetime of 3.78×10^{-6} sec. The fluorescently modified apo-enzyme (devoid of haem) HRP-C, showed an excited state lifetime of 4.23×10^{-6} sec duration, whilst that of free Ru complex I was found to be approximately 5×10^{-7} sec.

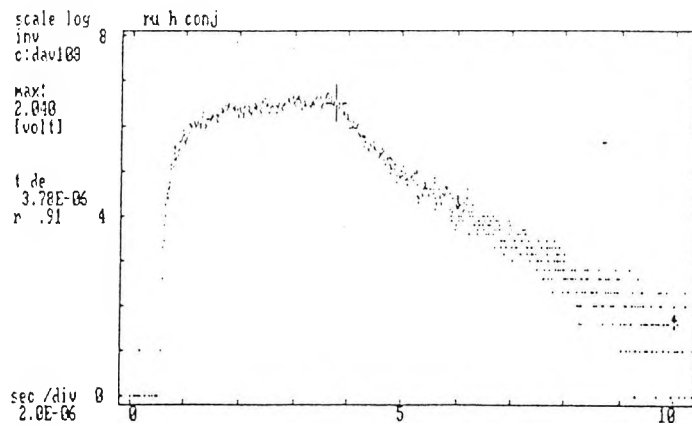


Fig. 8.12. Fluorescence decay curve for Ru Complex I/HRP-C Holo-enzyme (intact enzyme) conjugate.

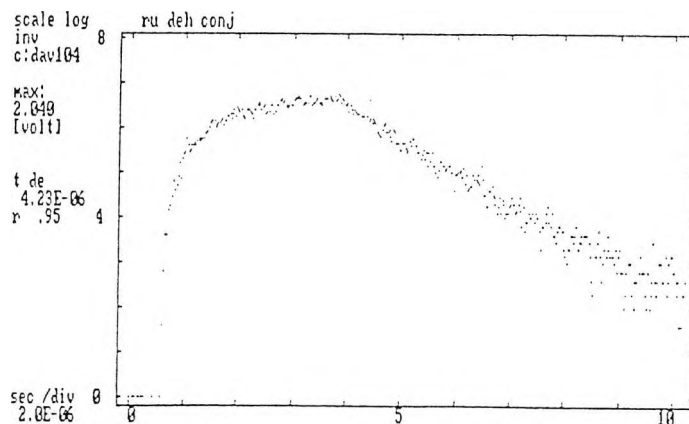


Fig. 8.13. Fluorescence decay curve for Ru Complex I/HRP-C Apo-enzyme (devoid of haem) conjugate.

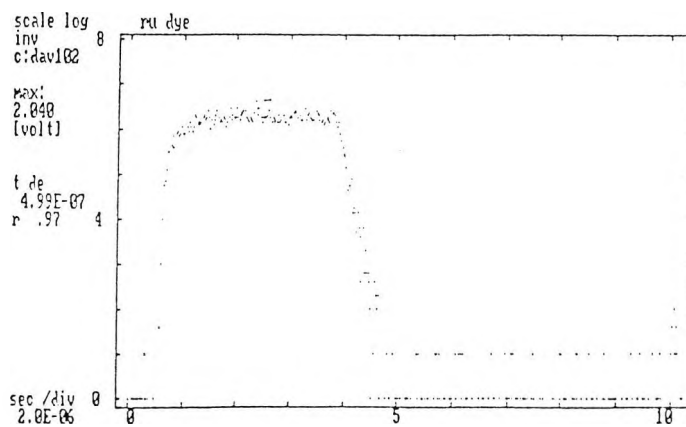


Fig. 8.14. Fluorescence decay curve for free Ru Complex I.

$$\begin{aligned}
E &= 1 - (T_{da}/T_d) \\
&= 1 - (3.78 \times 10^{-6}/4.23 \times 10^{-6}) \\
0.11 &= \frac{(13.6)^6}{(13.6)^6 + r^6} \\
r^6 &= 5.12 \times 10^7 \\
r &= \underline{19.27 \text{ \AA}}
\end{aligned}$$

8.10.3. Conclusion.

The distance, r , as determined by all three methods are in reasonable agreement, and the value obtained is feasible since the molecular radius of HRP-C is known to be 30 $\overset{\circ}{\text{A}}$ (50). We would expect the most reactive lysine residue to be present at a superficial location, and given the relationship between the protein and the haem moiety, it is likely that the latter is centrally located.

8.11. DETERMINATION OF THE POSITION OF THE REACTIVE LYSINE RESIDUE VIA AFFINITY CHROMATOGRAPHY.

Having established the distance between the haem centre and the reactive lysine residue, it would be advantageous to deduce which one of the six lysine residues is involved. An affinity chromatographic method for isolation, utilising an avidin-biotin derivative complex, was adopted.

8.11.1. Principle of Technique.

A remarkably strong non-covalent interaction between biotin (Vitamin H) and the egg-white protein, avidin,

(association constant, $K_D = 1 \times 10^{-15}$ M), allows for the purification of any molecule via affinity chromatography.

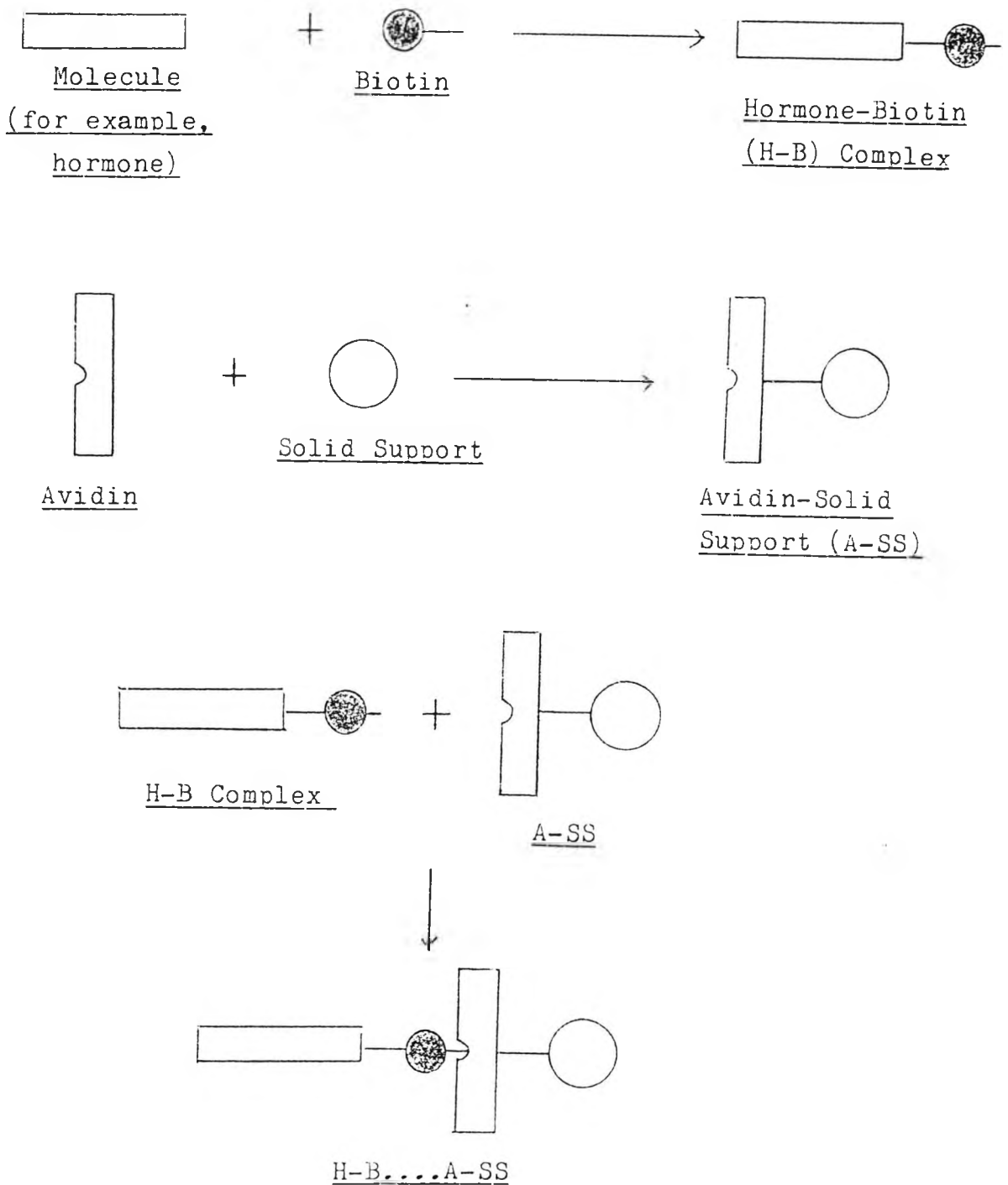


Fig. 8.15. Schematic representation of the principle of avidin-biotin affinity chromatography.

Subsequent removal of the biotin-bound molecule from the avidin-solid support, requires very harsh conditions and if the molecule to be isolated were a protein, destruction of the protein usually occurs. However, a more applicable method of affinity chromatography, utilising an avidin-biotin derivative complex, has been devised (54).

The basis of the technique is the covalent attachment of compounds containing 2-iminobiotin, the cyclic guanidino analogue of biotin, to the molecule under investigation. The pH-dependent interaction of 2-iminobiotin with avidin makes recovery possible. At high pH, the free base form of 2-iminobiotin retains the high affinity specific binding to avidin characteristic of biotin, whereas at acidic pH values, the salt form of the analogue interacts poorly with the avidin.

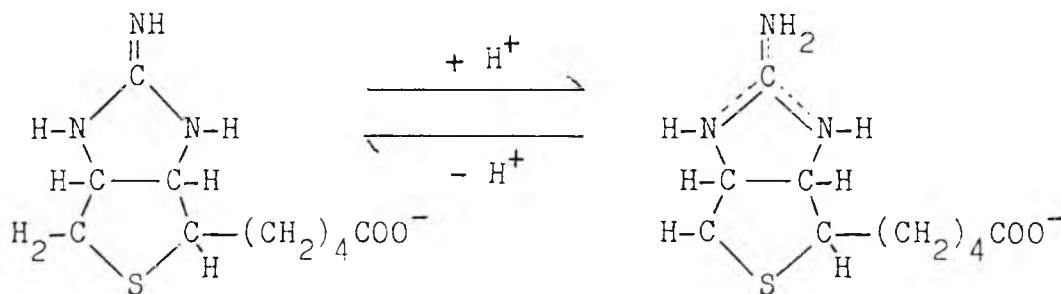


Fig. 8.16. Illustration of the pH-dependence of 2-iminobiotin.

For tight binding of the 2-iminobiotinylated molecule to the affinity matrix (avidin-solid support column), the pH of the column must be 9.5 or higher. Interaction is weak at low pH values, (less than pH 6.0). Elution from the affinity matrix may be accomplished at pH 4.0. It is thought that the reduction in binding efficiency of the 2-iminobiotin to avidin

at low pH, is a combination of the ionisations of the guanidino group of the analogue and an undetermined group on avidin.

8.11.2. Experimental Procedure.

Succinimidyl-2-iminobiotin (0.40 mg; 1.18 μ mol/mg protein) was utilised for the partial modification of Type III HRP-C (RZ value 3.2), as previously described in Section 8.8.1. The probe : protein ratio was found to be 1 : 1.

The purified conjugate was treated with aqueous urea (8.0 M, 50 μ l), and allowed to stand at room temperature, for 24 hours. 2-mercaptoethanol (50 μ l) was then added, and the mixture was allowed to stand, for a further 24 hours, at room temperature. Aqueous iodoacetic acid (0.05 M, 50 μ l) was then added, and the preparation was allowed to stand for yet another 24 hours, at room temperature.

The preparation was then dialysed extensively (3 days) against phosphate buffer (0.10 M, 1000 ml, pH 7.4), using cellulose tubing which retains molecular weight species in excess of 12000 daltons.

The conjugate was then subjected to enzymatic degradation employing an α -chymotrypsin preparation, rendered insoluble via covalent combination with carboxymethyl-cellulose. The protein preparation was stirred with the enzyme preparation, at room temperature, for 24 hours. Since α -chymotrypsin cleaves the peptide bond at specific positions, (carboxyl-terminal to an aromatic amino acid residue), it follows that the composition of the peptide fragments may be predicted.

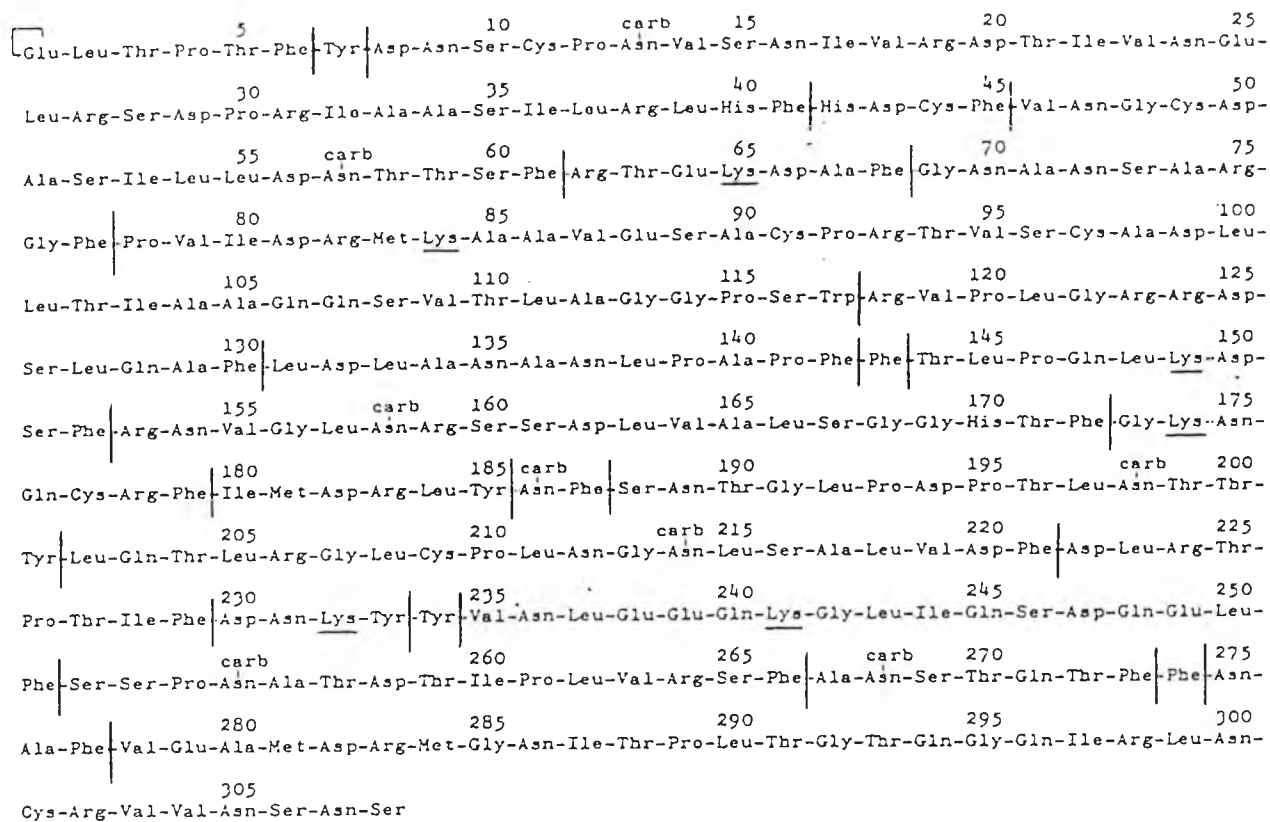


Fig. 8.17. The primary structure of HRP-C, indicating sites of enzymatic cleavage.

Lysine residues are present at positions 65, 84, 149, 174, 232 and 241. These residues are underlined.

Thus, it is expected that 27 peptide fragments are present. The enzymatic digest was then rendered basic (pH 10), by the addition of ammonium carbonate/ NH_4OH buffer (50 mM, pH 11) dropwise. An aliquot of this preparation (200 μl) was put onto a column of egg-white avidin, attached to acrylic beads, which had previously equilibrated with the ammonium carbonate/ NH_4OH buffer (bed volume: 3 ml). The column was eluted with excess ammonium carbonate buffer, and the issuing eluate was discarded. Ammonium acetate/ CH_3COOH buffer (50 mM, pH 3) was then added to the column. The pH of the issuing eluate was monitored, and on reaching pH 4.0, fractions (10 x 1 ml) were

collected.

Aqueous succinimidyl-2-iminobiotin was subjected to U.V./visible spectral analysis, and was found to absorb maximally at 204.6 nm. Fractions 6 and 7 were found to absorb maximally at 203.2 nm and 204.9 nm respectively, and these were combined, brought to pH 8.0 by the addition of aqueous sodium hydroxide (0.05 M) dropwise, and subjected to Fast Atom Bombardment Mass Spectroscopy.

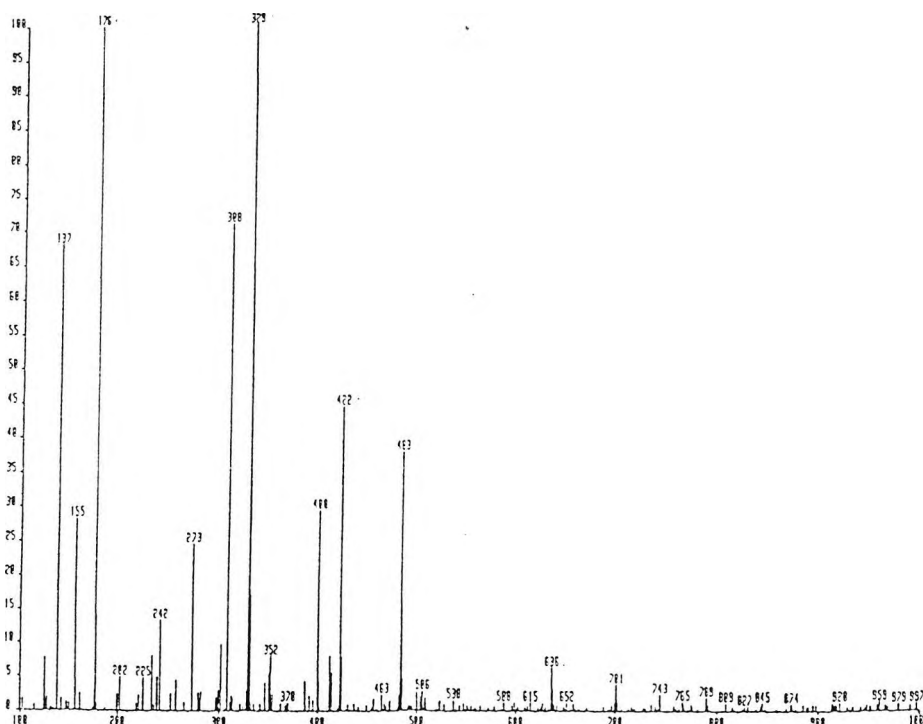
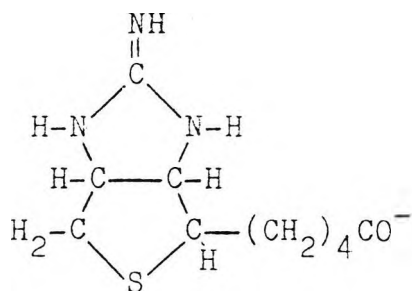
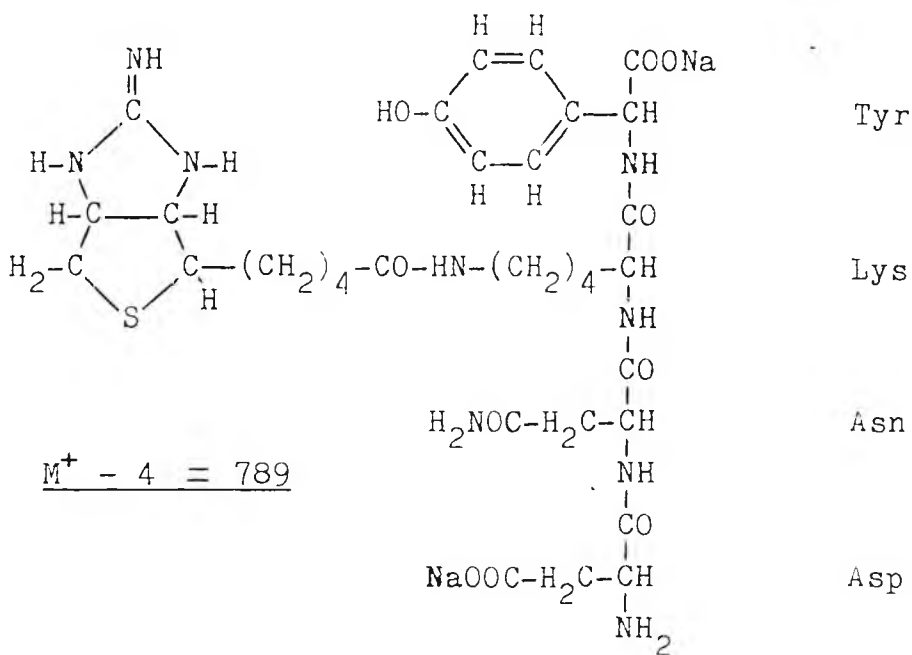


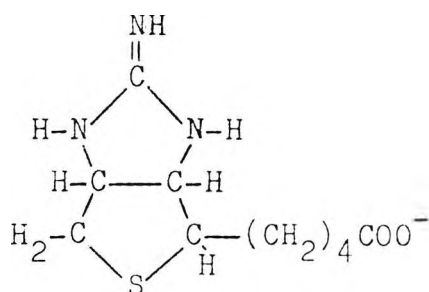
Fig. 8.18. Fast Atom Bombardment Mass Spectroscopic Print-out of 2-imino-biotinylated/HRP-C fragment.

8.11.3. Results.

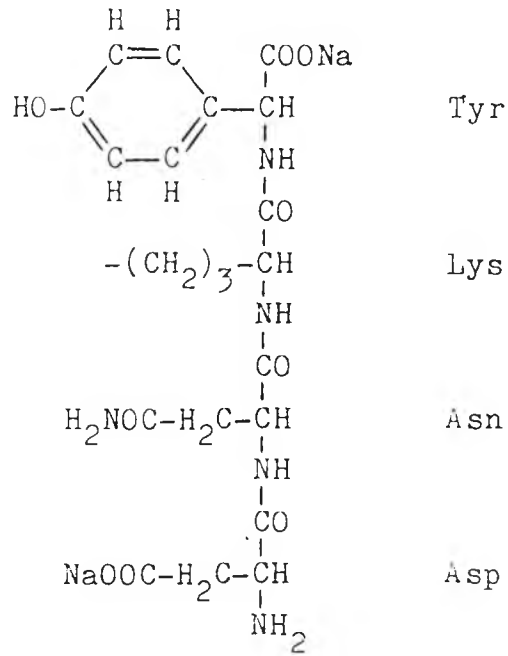
The peaks at molecular weights 176, 308, 329, 400, 422, 483 and 701, were ascribed to the interaction of sodium ions with the spectroscopic matrix.



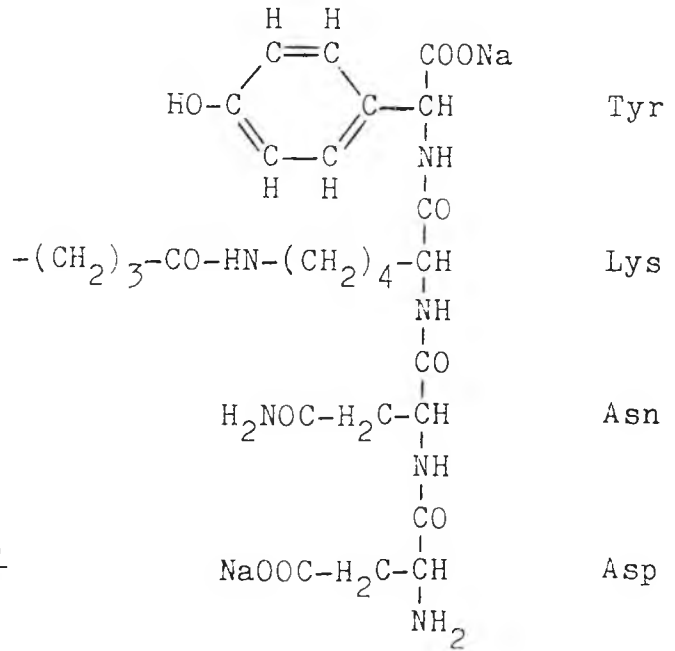
$$\underline{M^+ - 1 = 225}$$



$$\underline{M^+ = 242}$$

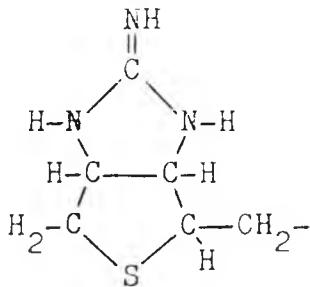


$$\underline{M^+ + 1 = 539}$$



$$\underline{M^+ - 1 = 636}$$

(plus one methylene
group = $M^+ + 1 = 652$)



$$\underline{M^+ - 1 = 155}$$

8.11.4. Conclusion.

In order for enzymatic cleavage to occur, the protein must be devoid of its higher structure. The use of aqueous urea serves to destroy areas of secondary structure, so that the polypeptide is stabilised only by disulphide linkages. addition of 2-mercaptoethanol reduces these disulphide linkages, so that thiol groups are formed. Subsequent removal of the urea and 2-mercaptoethanol would result in auto-oxidation of the thiol groups to disulphide bridges, and reorganisation of the protein to its original tertiary structure. The use of iodoacetic acid prevents this by conversion of the thiol groups to cysteic acid.

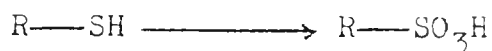


Fig. 8.19. Reaction for the preparation of cysteic acid.

Disulphide bridge re-formation cannot now occur, and therefore the preparation may be dialysed prior to enzymatic cleavage.

All of the eight glycosylated asparagine residues present in HRP-C, are found on a tripeptide sequence exhibiting glycosylated asparagine-X-Ser/Thr, where X may be any amino acid residue (but usually not proline). This sequence signals a reverse turn in the polypeptide backbone, and these occur on the surface of the protein molecule. It has been predicted (27), that only two lysine residues of HRP-C would be present on a polypeptide stretch comprising a reverse turn, and these were adjudged to be lysine residues at positions 174 and 232.

A hydrophathic index for the various amino acid residues present in HRP-C, TP-7 and CCP, has been compiled (27).

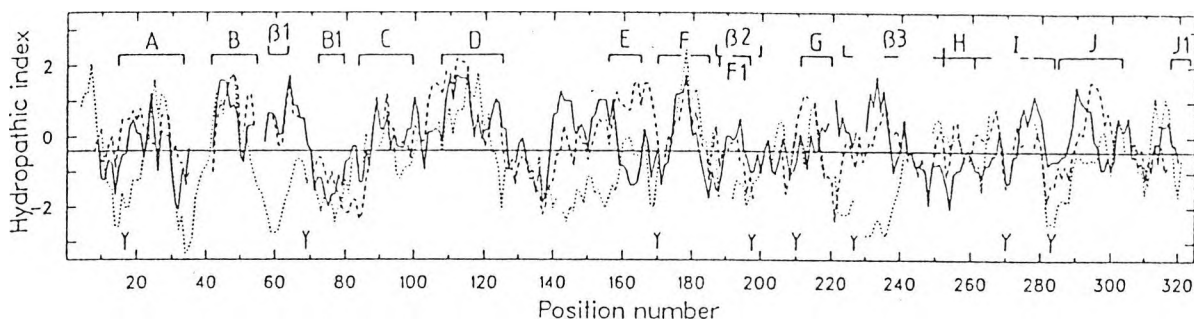


Fig. 8.20. Hydrophathic character along peroxidase sequences. Horseradish peroxidase HRP-C (—), turnip peroxidase TP-7 (- -), and cytochrome c peroxidase (...) are shown. Positive hydrophathy indicates hydrophobicity. Helices and extended structure observed in cytochrome c peroxidase and glycosylated sites in HRP-C (Y) are indicated (27).

Allowing for alignment gaps, lysine-174 appears to be located in a more hydrophobic environment than does lysine-232.

The mass spectral data indicate that the tetrapeptide spanning residues 230-233 inclusive, comprising aspartate-asparagine-lysine-tyrosine, is present in the sample, and therefore, it is suggested that lysine-232 is the amino acid residue implicated in the fluorescence quenching studies.

Thus, having determined the distance between the haem centre and the most reactive lysine residue, as well as suggesting that the latter is lysine-232, further information may be gained concerning the tertiary structure of the HRP-C molecule.

8.12. SUMMARY.

Horseradish peroxidase is a globular, plant haemoprotein of molecular radius $30 \overset{\circ}{\text{A}}$, obtained from horseradish roots. It is composed of at least twenty isoenzymes of which isoenzyme C is the most abundant. Isoenzymes A1 and C require calcium ions for catalytic activity.

Isoenzyme C comprises 308 amino acid residues, of which eight are glycosylated asparagine residues. The haem moiety is located between two polypeptide domains. The isoenzyme shares common primary sequences with turnip peroxidase and yeast cytochrome c peroxidase. All possess the iron protoporphyrin IX, or haem moiety, as their prosthetic group, which is attached to the protein via a histidine residue. As a consequence, these proteins exhibit similar secondary and tertiary structures.

However, the proteins differ in their catalytic activity. HRP is unusual in that the substrate does not make physical contact with the iron atom of the haem moiety. Instead, the substrate binds to the δ meso carbon atom of the porphyrin, and hydroxylation occurs at the 8-methyl position.

The HRP-C molecule was partially modified with a fluorescent amine-reactive agent, and the haem moiety was found to quench the fluorescence of the extrinsic fluorophore. The extent of the fluorescence quenching, allowed the calculation of the distance between the haem moiety and the attendant fluorophore. This distance was found to be in the range 17.51 to $19.27 \overset{\circ}{\text{A}}$.

Affinity chromatography studies suggested that the reactive lysine residue, was located at position 232.

8.13. REFERENCES.

1. Schönbein, C.F.
(1863) J. Prakt. Chem. 98 323
2. Bourquelot, E.
(1898) C.R. Soc. Biol., Paris 50 381
3. Linossier, G.
(1898) C.R. Soc. Biol., Paris 50 373
4. Willstätter, R. & Pollinger, A.
(1923) Liebigs Ann. 430 269
5. Theorell, H.
(1942) Ark. Mineral. Geol. No.2 16A
6. Paul, K.G.
(1958) Acta Chem. Scand. 12 1312
7. Shannon, L.M., Kay, E. & Lew, J.Y.
(1966) J. Biol. Chem. 241 2166
8. Shih, J.H.C., Shannon, L.M., Kay, E. & Lew, J.Y.
(1971) J. Biol. Chem. 246 4546
9. Theorell, H. & Maehly, A.C.
(1950) Acta Chem. Scand. 4 422
10. Whitehead, J.S., Kay, E., Lew, J.Y. & Shannon, L.M.
(1971) Anal. Biochem. 40 287
11. Keilin, D.
(1927) C.R. Soc. Biol., Paris (Reunion pleniere) 97 39
12. Kuhn, R., Hand, D.B. & Florkin, M.
(1931) Hoppe Seylers Zeitschrift für Physiol. Chemie 201 255
13. Elliott, K.A.C. & Keilin, D.
(1934) Proc. Roy. Soc. B 114 210
14. Sumner, J.B. & Howell, S.F.
(1936) Enzymologia 1 133
15. Keilin, D. & Mann, T.
(1937) Proc. Roy. Soc. B 122 119
16. Keilin, D. & Hartree, E.F.
(1951) Biochemical J. 49 88

17. Herbert, D. & Pinsent, J.
(1948) *Biochemical J.* 43 193
18. Delincee, H. & Radola, B.J.
(1970) *Biochim. Biophys. Acta* 200 404
19. Cecil, R. & Ogston, A.G.
(1951) *Biochemical J.* 49 105
20. Haschke, R.H. & Friedhoff, J.M.
(1978) *Biochem. Biophys. Res. Commun.* 80 1039
21. Welinder, K.G.
(1979) *Eur. J. Biochem.* 96 483
22. Welinder, K.G.
(1976) *FEBS Letters* 72 19
23. Welinder, K.G. & Smillie, L.B.
(1972) *Can. J. Biochem.* 50 63
24. Lesk, A.M. & Chothia, C.
(1980) *J. Mol. Biol.* 136 225
25. Morrison, M. & Schonbaum, G.R.
(1976) *Ann. Rev. Biochem.* 45 861
26. Takio, K., Titani, K., Ericsson, L.H. & Yonetani, T.
(1980) *Arch. Biochem. Biophys.* 203 615
27. Welinder, K.G.
(1985) *Eur. J. Biochem.* 151 497
28. IUPAC-IUB Joint Commission on Biochemical Nomenclature
(1984) *Eur. J. Biochem.* 138 9
29. Strickland, E.H., Kay, E., Shannon, L.M. & Horwitz, J.
(1968) *J. Biol. Chem.* 243 3560
30. Job, D. & Dunford, H.B.
(1977) *Can. J. Biochem.* 55 804
31. Hamaguichi, K., Ikeda, K., Yoshida, C. & Morita, Y.
(1969) *J. Biochem. (Tokyo)* 66 191
32. Poulos, T.L., Freer, S.T., Alden, R.A., Edwards, S.L., Skogland, U., Takio, K., Ericsson, B., Xuong, N., Yonetani, T. & Kraut, J.
(1980) *J. Biol. Chem.* 255 575

33. Dunford, H.B. & Stillman, J.S.
(1976) *Coord. Chem. Rev.* 19 187
34. Poulos, T.L., Finzel, B.C., Gunsalus, I.C., Wagner, G.C.
& Kraut, J.
(1985) *J. Biol. Chem.* 260 16122
35. Ortiz de Montellano, P.R. & Grab, L.A.
(1987) *Biochemistry* 26 5310
36. Kedderis, G.L., Rickert, D.E., Pandey, R.N.
& Hollenberg, P.F.
(1986) *J. Biol. Chem.* 261 15910
37. Ortiz de Montellano, P.R., Choe, Y.S., DePillis, G.
& Catalano, C.E.
(1987) *J. Biol. Chem.* 262 11641
38. Kobayashi, S., Nakano, M., Goto, T., Kimura, T.
& Schaap, A.P.
(1986) *Biochem. Biophys. Res. Commun.* 135 166
39. Kobayashi, S., Nakano, M., Kimura, T. & Schaap, A.P.
(1987) *Biochemistry* 26 5019
40. Ator, M.A. & Ortiz de Montellano, P.R.
(1987) *J. Biol. Chem.* 262 1542
41. Ringe, D., Petsko, G.A., Kerr, D.E.
& Ortiz de Montellano, P.R.
(1984) *Biochemistry* 23 2
42. Augusto, O., Kunze, K.L. & Ortiz de Montellano, P.R.
(1982) *J. Biol. Chem.* 257 6231
43. Ortiz de Montellano, P.R., Kunze, K.L. & Augusto, O.
(1982) *J. Amer. Chem. Soc.* 104 3545
44. Ortiz de Montellano, P.R. & Kerr, D.E.
(1983) *J. Biol. Chem.* 258 10558
45. Jonen, H.G., Werringloer, J., Prough, R.A. & Estabrook, R.W.
(1982) *J. Biol. Chem.* 257 4404
46. Santimone, M.
(1975) *Biochimie (Paris)* 57 265
47. Ugarova, N.N., Rozhkova, G.D., Vasileva, T.E. & Berezin, I.V.
(1978) *Biochimiya* 43 793

48. Teale, F.W.J.
(1959) *Biochim. Biophys. Acta* 35 543
49. Chen, R.F.
(1969) *Arch. Biochem. Biophys.* 133 263
50. Rennke, H.G. & Venkatachalam, M.A.
(1979) *J. Histochem. Cytochem.* 27 1352
51. Johnson, D.A., Voet, J.G. & Taylor, P.
(1984) *J. Biol. Chem.* 259 5717
52. Parker, C.A. & Rees, W.T.
(1960) *Analyst* 85 587
53. Jasiewicz, M.L., Schoenberg, D.R. & Mueller, G.C.
(1976) *Exp. Cell. Res.* 100 213
54. Orr, G.A.
(1981) *J. Biol. Chem.* 256 761

APPENDIX.

EXPERIMENTAL DETAILS.

EXPERIMENTAL DETAILS.

All chemicals were of reagent grade, and were obtained commercially, unless otherwise stated.

Stock CRP solution was supplied by SmithKline Beecham Pharmaceuticals in PBS (0.10 M) containing glycerol (50% v/v).

All other proteins were obtained commercially, unless otherwise stated.

Instruments Used for the Recording of Spectra.

Infra-red : Recorded on a Perkin-Elmer 983G Infra-red Spectrophotometer.

Fluorescence : Recorded on a Perkin-Elmer MPF-4 Spectrophotometer.

Ultra-violet : Recorded on a Perkin-Elmer Lambda-5 U.V./visible Spectrophotometer.

¹H n.m.r. : Recorded on a Jeol JNM-PMX-60 (60 MHz), employing tetramethylsilane as the internal standard.

Mass Spectra : Recorded on a Kratos MS30 (electron impact), operated by Mr. Chris Whitehead.

FAB Mass Spectra : Recorded at the SERC Mass Spectrometry Service Centre, University College of Swansea.

Instruments Used for the Measurement of Other Parameters.

Luminescent Lifetimes : Recorded using a helium-cadmium laser Model 4240NB, incorporating a Carl Zeiss LAB 16 Fluorescence Microscope.

Microanalysis : Performed on Carlo-Erba Model 1106 Elemental Analyser.

Melting Points : Recorded on Griffin Melting Point Apparatus Serial No. P1158.

Gel Electrophoresis : Performed on Bio-rad Gel Electro-
phoresis Cell, Model 150A, utilising
a Bio-rad Model 500 Power Supply Unit.

Thin-Layer Chromatography : Performed on Silica-gel Plates.

Protocols for the Preparation of Aqueous Buffers.

Carbonate Buffer (0.05 M), composed of NaHCO_3 (2.10 gm),
 NaOH (1.00 gm) per 1000 ml distilled water.

Phosphate Buffered Saline (0.10 M, PBS), composed of
 Na_2HPO_4 (7.10 gm), KH_2PO_4 (6.80 gm) containing NaCl (0.90% w/v),
per 1000 ml distilled water, adjusted to pH 7.4 with NaOH .

Phosphate Buffer, as utilised, was devoid of NaCl .

HEPES (N-2-Hydroxyethylpiperazine-N'-2-ethanesulphonic acid)/
 KCl (0.50 M), composed of HEPES (4.76 gm), KCl (37.25 gm)
per 1000 ml distilled water, adjusted to pH 7.4 with KOH .

Tris-HCl (Tris(hydroxymethyl)-aminomethane hydrochloride)/
 KCl /EDTA (Ethylenediamine N,N,N',N'-tetra-acetic acid) (0.20 M),
composed of Tris-HCl (3.16 gm), KCl (14.90 gm), EDTA (0.03 gm)
per 1000 ml distilled water, adjusted to pH 8.0 with KOH .

Tris-HCl/ KCl / MgCl_2 /dithiothreitol (0.20 M), composed of
Tris-HCl (7.90 gm), KCl (11.18 gm), MgCl_2 (0.95 gm),
dithiothreitol (0.015 gm) per 1000ml distilled water,
adjusted to pH 8.0 with KOH .

Tris-HCl/ KCl Buffer, as utilised, was devoid of MgCl_2
and dithiothreitol.

Tris-HCl Buffer (0.375 M), composed of Tris-HCl (59.25 gm)
per 1000 ml distilled water, adjusted to pH 8.8 with KOH .

Tris-HCl Buffer (0.125 M), composed of Tris-HCl (19.75 gm)
per 1000 ml distilled water, pH 6.8.

Tris-HCl Buffer (0.025 M), composed of Tris-HCl (3.95 gm)
per 1000 ml distilled water, adjusted to pH 8.3 with KOH .